sustainability

MDPI

Article

Assessing the Prospects of Transboundary Multihazard Dynamics: The Case of Bhotekoshi–Sunkoshi Watershed in Sino–Nepal Border Region

Suraj Lamichhane [1,2], Komal Raj Aryal [3,*], Rocky Talchabhadel [2,4], Bhesh Raj Thapa [2,5,6], Rabindra Adhikari [2,7], Anoj Khanal [8], Vishnu Prasad Pandey [1,2] and Dipendra Gautam [2,6,7,9,*]

1 Department of Civil Engineering, Institute of Engineering, Pulchowk Campus, Tribhuvan University, Lalitpur 44601, Nepal; surajlamichhane@ioe.edu.np (S.L.); vishnu.pandey@pcampus.edu.np (V.P.P.)
2 Interdisciplinary Research Institute for Sustainability (IRIS), Kathmandu 44600, Nepal; rocky.talchabhadel@ag.tamu.edu (R.T.); bthapa.ioe@gmail.com (B.R.T.); rabindraadhi@cosmoscollege.edu.np (R.A.)
3 Faulty of Resilience, Rabdan Academy, Abu Dhabi 114646, United Arab Emirates
4 Texas A&M AgriLife Research, Texas A&M University, El Paso, TX 79927, USA
5 Department of Civil Engineering, Universal Engineering and Science College, Lalitpur 44601, Nepal
6 Nepal Academy of Science and Technology, Lalitpur 44601, Nepal
7 Department of Civil Engineering, Cosmos College of Management and Technology, Lalitpur 44601, Nepal
8 Kathmandu Valley Water Supply Management Board, Lalitpur 44601, Nepal; geologistkhanal@gmail.com
9 Department of Civil Engineering, Institute of Engineering, Thapathali Campus, Tribhuvan University, Kathmandu 44600, Nepal
* Correspondence: karyal@ra.ac.ae (K.R.A.); dipendra01@tcioe.edu.np (D.G.)

Citation: Lamichhane, S.; Aryal, K.R.; Talchabhadel, R.; Thapa, B.R.; Adhikari, R.; Khanal, A.; Pandey, V.P.; Gautam, D. Assessing the Prospects of Transboundary Multihazard Dynamics: The Case of Bhotekoshi–Sunkoshi Watershed in Sino–Nepal Border Region. *Sustainability* **2021**, *13*, 3670. https://doi.org/10.3390/su13073670

Academic Editor: Andrzej Wałęga

Received: 21 February 2021
Accepted: 17 March 2021
Published: 25 March 2021

Abstract: The impacts of multihazards have become more pronounced over the past few decades globally. Multiple hazards and their cascading impacts claim enormous losses of lives, livelihoods, and built environment. This paradigm prompts integrated and multidisciplinary perspectives to identify, characterize, and assess the occurrence of multihazards and subsequently design countermeasures considering impending multihazard scenarios at the local level. To this end, we considered one of the most egregious transboundary watersheds, which is regarded as a multihazard hotspot of Nepal, to analyze the underlying causes and cascade scenarios of multihazards, and their associated impacts. In this paper, geophysical, hydrometeorological, and socioeconomic perspectives are formulated to characterize the watershed from the dimension of susceptibility to multihazard occurrence. To characterize the complex dynamics of transboundary multihazard occurrence, insights have been presented from both the Nepali and the Chinese sides. Individual case studies and the interrelation matrix between various natural hazards are also presented so as to depict multihazard consequences in the transboundary region. The sum of the observations highlights that the watershed is highly vulnerable to a single as well as multiple natural hazards that often switch to disasters.

Keywords: Bhotekoshi–Sunkoshi watershed; geophysical hazard; hydrometeorological hazard; multihazard; socioeconomy

1. Introduction

Environmental disasters are quite frequent in Nepal and due to young geology, topography, location of settlements, lack of proper settlement planning, and limited preparedness initiatives, most of the natural hazards become disasters. The United Nations Development Program (UNDP) designates Nepal as the 20th most vulnerable country in terms of multihazards, 4th most vulnerable in terms of climate change-related hazards, 11th in terms of earthquake hazards, and 30th in terms of flood-related hazards [1]. The frequency of environmental disasters has increased over the past few decades in Nepal [2]. The enormous losses in terms of lives, lifelines, and others are well documented in Nepal,

especially after 2000, and thus provide a notable background to assess and understand the dynamics of multiple natural hazards across the country. It is worthy to note that some parts of the country observe more frequent disaster incidents than others. To be precise, some districts in Nepal are hotspots for multiple natural hazards and associated disasters so that the losses are not homogenous throughout the country. Furthermore, the population of the country is greatly heterogeneous, with the mountains almost uninhabited and the southern plains and some valleys overly populated. To this end, the disaster impacts in Nepal are mostly localized, as reported by Aryal [3]. Studies related to the occurrence, impacts, and insights from historical disasters are emerging in Nepal; however, most of such studies have focused on earthquakes [4,5], floods [6–8], glacial lake outburst floods (GLOF) [9,10], and landslides [11,12]. On the other hand, other natural hazards, such as thunderstorms, windstorms, avalanches, and drought, among others, have received relatively less attention [13,14]. Several independent natural hazards are incorporated in the published literature; however, to the best of the authors' knowledge, integrated multihazard studies are very limited in Nepal [15–17]. Due to the changing climate, the multifaceted challenges of independent and multiple natural hazards and their association with cascading impacts would be further pronounced in the future. To this end, we fully recognize the multifaceted impacts of climate change on multiple socioeconomic sectors that are reported elsewhere [11,18].

The global understanding in terms of multihazard challenges has taken a more streamlined trajectory. Studies on frameworks, applications, and policy interventions for multihazards have been widely developed so far on the global scale. Most of the existing literature incorporates multihazard risk assessment of infrastructures [19–21]; whereas, quite a few studies consider multihazard impacts on built environment on a societal scale [22–24]. The changing landscape of infrastructure construction and social vulnerability widely depends on the occurrence and consequences of multihazards. To this end, global attention has focused more on integrated hazards for disaster preparedness. For countries exposed to multiple hazards, there is an urgent need to identify location-specific frequently occurring environmental hazards and induced disaster incidents. Examples include the 2015 Gorkha earthquake in Nepal that claimed 8790 lives with USD 7 billion losses [25]; the 2017 flood events in Nepal that claimed a total loss of USD 187.9 million [26], and the 2020 flood and landslides that claimed over USD 350 million [2]. This evidence clearly portrays that the impacts of the independent natural hazard-induced disasters, repeating in the same location, are very high in Nepal. Moreover, several examples demonstrate that frequent multiple disasters strike in the same region and lead to enormous losses of lives and properties. This notion demands studies related to the assessment of multihazard risk on a local scale. Apart from multihazard issues on a regional and national scale, some critical aspects of transboundary multihazard dynamics cannot be undermined due to their instrumental presence in terms of managing the common problems between two or more countries. To have an effective mechanism and negotiations, characterization of multihazard vulnerability beyond the border is the first step towards integrated initiatives as discussed by several researchers [27–29]. To the best of authors' knowledge, such studies are missing in the existing literature. To fulfill the hiatus, we performed a two-layered analysis considering one of the egregious neighborhoods, the Bhotekoshi–Sunkoshi Watershed (BSW) corridor, in central Nepal in the Sino–Nepal border region. The multihazard cascading and independent scenarios in the transboundary region are formulated, and some case studies of historical natural hazards are also presented in this paper.

2. Study Area

The BSW above the confluence with Balefi River (located outside the boundary of the BSW as shown in Figure 1) covers an area of 2558 km^2 that extends between 27°42′41″–28°31′05″ N latitude and 85°42′59″–86°19′37″ E longitude (Figure 1). Of the total catchment area, 22.5% lies in Nepal and the rest in the Tibet autonomous region of China. The climate in the BSW varies from temperate to polar [30]. Administratively, there are six Palikas

(local administrative units) that fall partially or fully within this portion of the BSW in Nepal (Figure 1, Table 1). They are Bhotekoshi, Bahrabise, Sunkoshi, Balefi, Tripurasundari, and Lisangkhu Pakhar. The proportion of the Palika area within the watershed is shown in Table 1.

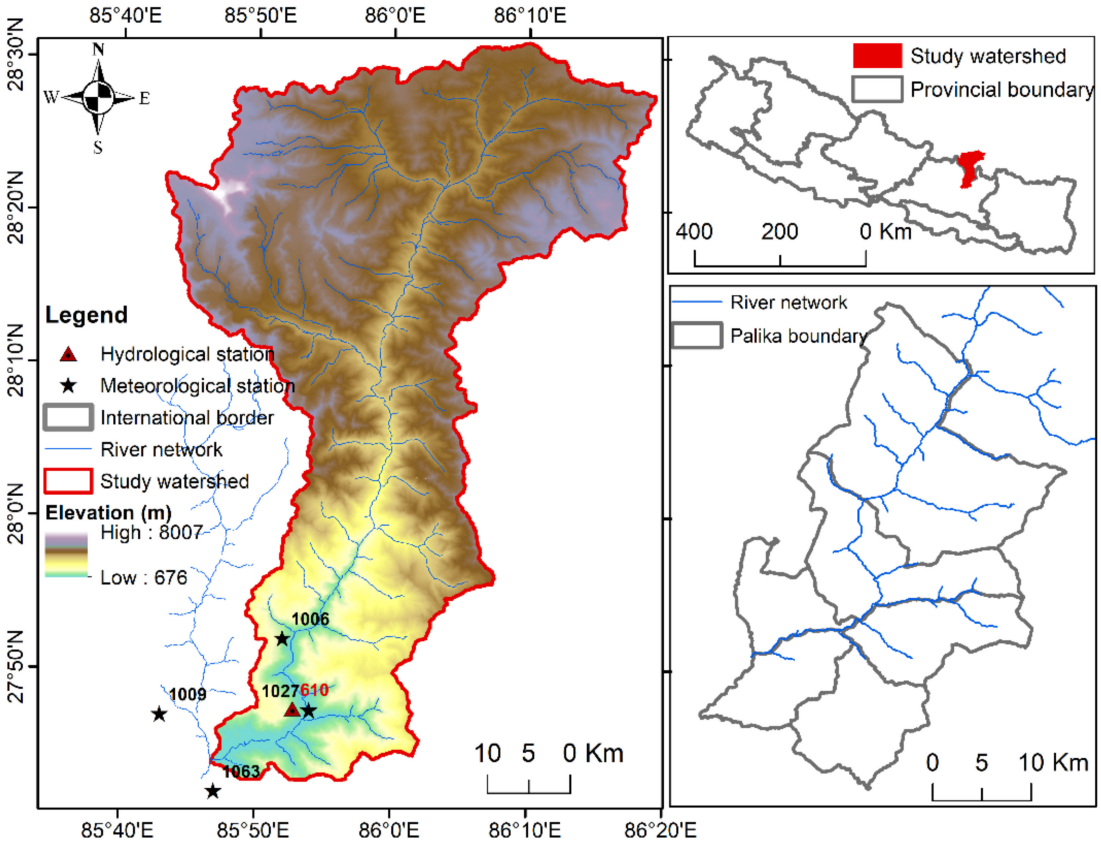

Figure 1. Location, topographic, and administrative details of the Bhotekoshi–Sunkoshi watershed.

Table 1. Proportion of Palika (local administration) area within the Bhotekoshi–Sunkoshi watershed.

Name of Palika	Total Area of Palika (km^2) Calculated from GIS Shapefile	% of Area within the Watershed
Bhotekoshi	278.04	100
Bahrabise	134.68	100
Sunkoshi	72.8	25
Balefi	61.57	29
Tripurasundari	94.2	88
Lisangkhu Pakhar	98.54	6

3. Methodology

We carried out rigorous literature reviews to identify the various aspects of watershed characteristics that trigger and/or influence multiple natural hazards and contribute to associated vulnerabilities in the watershed. This resulted in five aspects of primary importance, viz., topographical, geological, hydrometeorological, glacial lakes (existence and spread), and socioeconomy. Further review was focused on identifying a suitable set of indicators/parameters to characterize these five aspects and establishing their logical link to multiple natural hazards and associated vulnerabilities. The five aspects, their indica-

tors/parameters, and associated logical links to multiple natural hazards (independent or cascading) are shown in Table 2 and elaborated in the following subsections.

Table 2. A framework developed for watershed characterization from multihazard perspectives.

Watershed Characteristics	Indicator/Parameter	Logical Link to Multiple Hazards	Reference(s)
Topographical	Elevation	Spatial distribution of topography affects distribution of floods, with flat area prone to more flooding	[31]
	Slope	Damage potential due to natural hazards such as landslide is high in flat topography than in steep topography	[31]
	Aspect	Influences/triggers landslide	[32]
	River density	Distribution of drainage density can play a role in reducing flood water as well as induce flooding depending upon location	[31]
Geological	Geological setting	Regional geological and geomorphological setting plays a significant role for the occurrence of geohazards in its preparatory phases	[33]
	Geostructure and lithology	Fault structure, lithological variation, sediment thickness and rock fracturing impact the occurrence of geohazards	[34]
Hydrometeorological	Rainfall	Rainfall infiltration may increase degree of saturation of soil, reduces soils shear strength, and ultimately may lead to occurrence of geohazards	[32,33]
	River flow	High flow may lead to flooding and excessively low flow may lead to drought	[34,35]
Glacier lakes	Erosion and sediment (entrainment of loose solid) in the watershed	Glacial lake outburst floods (GLOFs) evolve into debris flows by erosion and sediment entertainment, which increase peak discharge and volume leading to destructive damage in downstream	[36]
	Lake volume	Higher volume may lead to potential flood magnitude during GLOFs and vice versa	[36,37]
Socioeconomic	Socioeconomic variables	Population comprising significant number of people above 60 years and below 14 years will be more affected during disaster. Disasters will affect poor and physically disadvantaged people more than normal people and people with better economic status.	[3,38]

3.1. Topographical Characterization

The following four parameters are considered for topographical characterization, as used in other studies such as Lyu et al. [31] and Alkhasawneh et al. [32].

3.1.1. Elevation

This refers to the altitude of a location above the mean sea level. The distribution of elevation in the study watershed was extracted from a digital elevation model (DEM) of 30 m resolution (available at https://www.eorc.jaxa.jp/ALOS/en/aw3d30/index.htm (accessed on 17 March 2021)) using GIS. A hypsometric curve was also developed to further characterize topographical variations in the watershed.

3.1.2. Slope

Slope angle (degree) is the angle measured between a horizontal plane at a given point on the land surface. The slope was extracted from DEM using the surface analysis tool in GIS. The aspect was divided into five classes: <5°, 5–10°, 10–20°, 20–30°, 30–50°, and >50°.

3.1.3. Aspect

Slope aspect refers to the direction of the slope. The aspect map was developed based on DEM using surface analysis tools in GIS. The slope aspects are divided into nine classes, viz., flat, north, northeast, east, southeast, south, southwest, west, and northwest.

3.1.4. River density

This refers to the length of the water channel per unit area and was derived using a source radius of 1 km as suggested by Lyu et al. [31].

3.2. Geological Characterization

The geological characteristics of any basin have great significance on the occurrence, intensity, and effects of multiple geohazards. To understand the geological setting and complexities of the study area, regional scale geological maps were reviewed and modified thoroughly. Information on the major rock type, lithological units, and major thrusts were gathered from published literature [33,35] and overlaid with major landslide events [39] using GIS. Major historical seismic events were thoroughly reviewed and analyzed to correlate the effect of seismic events on the occurrence of multiple geohazards, especially landslides and landslide dam outburst flood (LDOF).

3.3. Hydrometeorological Characterization

There are only two precipitation stations (station no. 1006 and station no. 1027) located within the study watershed and two other precipitation stations (station no. 1009 and station no. 1063) are located nearby the watershed. These stations administered by the Department of Hydrology and Meteorology (DHM) are not sufficient to characterize the entire study area. Similarly, there is only one station for temperature where the data are available only since 2011. The upper region of the watershed is located in China. To include the spatial diversity of the precipitation and temperature, we used gridded data. For temperature, we used the monthly climatic normal data (1970–2000) from the WorldClim version 2.1, available online (http://worldclim.org (accessed on 17 March 2021)) [40], at different spatial resolutions varying from 1 km to 20 km. The WorldClim gridded data has been widely used in many disciplines all over the world including Nepal. Talchabhadel and Karki [41] conducted a performance analysis of WorldClim data for different elevation bands across the country and reported that the products are useful for characterizing the climate at any location, though only the normal data are available. We used the temperature data of resolution ~5 km to make it consistent with the gridded precipitation product used in this study. For precipitation, we used the daily data of CHIRPS (Climate Hazards Group Infrared Precipitation with Stations) [42], which is a blending of satellite and gauge precipitation data and available since 1981 at a spatial resolution of ~5 km. We compared the performance of CHIRPS data at those four DHM stations before utilizing the data for the entire area. Detailed information on these performance metrics is available in [43]. We used precipitation events detection indices, such as the probability of detection, false alarm ratio, critical success index, and frequency bias index. They show that CHIRPS could detect the precipitation event with the probability of >0.6, with a critical success index of >0.5, and the frequency bias index nearly equals 1. However, there were a few false alarms of about 0.4. We also computed root mean square error (RMSE) and percentage bias (PBIAS) with respect to the observed precipitation data on a daily scale. The values of RMSE are less than 10 mm/day, and the PBIAS values range from 88% to 109%, indicating the overall magnitudes are well captured. In total, 252 grid points were used for this study, among them 92 grid points are located inside the study area. For the calculation of basin-averaged value, we used 92 grid points, whereas for the representation of the spatial map we used all 252 points. Point to raster at a resolution of 5 km was used in GIS platform to develop spatial maps for precipitation amounts and different extreme precipitation indices.

For each grid point, the maximum one-day precipitation of the year (RX1day) and the number of days in a year with daily rainfall $\geq$50 mm (R50) were computed. The RX1day is an absolute index, whereas the R50 is the threshold-based index. We also computed the RX7day (maximum consecutive seven-day precipitation in a year). Different floods (riverine and flash floods) and sediment hazards (soil erosions, landslides, and debris flow) occur during the instances of RX1day and RX7day, and mostly during the days when daily precipitation $\geq$50 mm. The annual values were then averaged for different four decades and for an entire period (1981–2019) to compute decadal and entire period precipitation amounts (annual) and extreme precipitation indices (RX1day, RX7day, and R50).

For hydrological characterization, we analyzed average annual and seasonal discharges derived from daily streamflow data at Bahrabise hydrological station (index: 610),

operated by DHM and located 15 km upstream of the BSW outlet. The daily streamflow data is based on the average of three time readings at 8 am, noon, and 4 pm. This is the highest resolution data publicly available from the DHM [43]. Flood frequency analysis was carried out of instantaneous maximum flood time series.

3.4. Glacial Lakes Characterization

Glacial lake outburst floods (GLOFs) are the major concern in the Himalayas in recent decades due to associated disasters and significant loss of lives, infrastructures, and properties. In this context, the characterization of glacial lakes and their distribution is crucial to understand the susceptibility to GLOF related disasters. In this study, the disasters occurring over the past century, glaciers and their sizes and distributions were reviewed from the past literature [36]. In addition to this, the glacial lakes and their severity were mapped in ArcGIS using a recent dataset available from the study by [36].

3.5. SocioEconomic Characterization

The socioeconomic characterization of the watershed was derived from the 2011 census and local administration units' profiles. Using the secondary data collected by the Central Bureau of Statistics, Government of Nepal [44] and the local administrations, socioeconomic characterization comprises gender, poverty, population, and disadvantaged population, among others to draw the confluence line in terms of the multihazard impacts and the socioeconomic settings. As watershed level data were not available for most of the local administrative units, district level interpretations are made due to the fact that the relative variation is not significant. The socioeconomic indicators have been interlinked with the likelihoods and impacts of the multihazard scenarios.

3.6. Data and Sources

Table 3 provides details of the data, their characteristics, and sources used in this study. Information regarding the type of data, sources, and their characteristics were postulated first to characterize multihazard impacts as the assessment o thef multihazard risk commences with the characterization of the governing factors.

Table 3. Characteristics and sources of data used in this study.

Data Type	Description/Characteristics	Data Source
Digital elevation model (DEM)	Raster data of 30 m horizontal resolution	Advanced Land Observing Satellite (ALOS) World 3D-DEM (AW3D)
River discharge	Daily river discharge (m^3/s) and instantaneous discharge (m^3/s) at Bahrabise station (index: 610; Lat.: 27°47′18″; Lon.: 85°53′55″) for the period of 1965–2006.	Department of Hydrology and Meteorology (DHM), Government of Nepal
Precipitation	Daily time series data at every 5 km spatial resolution	CHIRPS (Climate Hazards Group Infrared Precipitation with Stations)
Geology	Geological map of Nepal with major lithological units and faults	Department of Mines and Geology, Government of Nepal
Glacier lakes	Glacial lake inventory of Bhotekoshi based on GAoFEn-1 (GF-1) satellite image (http://www.cresda.com/CN/ (accessed on 17 March 2021))	[36]
Socioeconomic data	2011 National Housing and Population Census	Central Bureau of Statistics, Government of Nepal

4. Multihazard Susceptibility in Bhotekoshi–Sunkoshi Watershed

Susceptibility to multihazards depends on various factors that contribute in cascading events. Moreover, some scenarios usually occur in such a way that multiple events occur one after another, thereby aggravating the disaster impacts. This section outlines various features that trigger individual natural hazards or trigger some other natural hazards after one or more prevail.

4.1. Topographical Aspects of Multihazards

Topography has critical influence on the development and redistribution of various hazards. For example, the spatial distribution of the topography significantly affects the distribution of the flooding hazards [45] with flat areas prone to more flooding, variations in altitude create temperature and climate extremes. Natural hazards, such as landslides accompanied by debris flow and floods, can cause considerably less damage and fewer losses in flat topography than in the steep areas. Similarly, slope aspect has a link to natural hazards, in particular, landslide [32,46]. The distribution of drainage systems plays an important role in the reduction of floodwaters during flood events; however, it can also induce flooding [31,47]. Therefore, four parameters, viz., elevation, slope, aspect, and river density are considered as for the prime factors for topographical characterization.

The key topographical features of the watershed are presented in Table 4 and spatially distributed map of the four topography related parameters are shown in Figure 2. The elevation of the watershed varies widely between 676 to 8007 meters above sea level (m asl) (Figure 2a). About 18.3% of the watershed area lies below 3000 m asl and 39.2% of the area lies above 5000 m asl, as indicated in the hypsometric curve (Figure 3). The 3000 m and 5000 m elevations correspond roughly to the lower boundary of the snow line and the limit of the perennial snow and ice accumulation area. The zone below 3000 m is the zone of predominant monsoon rainfall (or the rain-fed zone).

Table 4. Main topographical features of the three watersheds in which the Madhya Bhotekoshi hydropower project has installed discharge gauging stations.

Features	Unit	Value
Catchment area (A)	km^2	2558
Area below 3000 m	km^2	467.5
Area between 3000 to 5000 m	km^2	880.4
Area above 5000 m	km^2	1002.1
Longest flow path (L)	km	145.3
Maximum elevation (Zmax)	m asl	8007
Minimum elevation (Zmin)	m asl	676
Mean elevation (Zmean)	m asl	4333
Average slope of river ((Zmax−Zmin)/L)	-	0.05

The slope of the watershed ranges from 0 to 88.2° (Figure 2b) and the average slope of the watershed is 5.0% (Table 4). The areas under different slope classes, as shown in Table 5, indicate that the vast majority (i.e., 82.1%) of the watershed area falls within the slope of 10° to 50°. In terms of the slope direction, all nine aspects are available in the watershed with their spatial distribution as shown in Figure 2c. Flat land is rare in the watershed (~0.1% of the watershed area only); however, all other eight aspects have somehow comparable proportions, i.e., they range from 11.3% to 13.9% (Table 5). In terms of the drainage density, it varies from 0 to 536 m/km^2. Most of the watershed areas (i.e., 64.3%) have z drainage density of less than 50 m/km^2, followed by that of 100–200 m/km^2 (15.7% of watershed area) as shown in Table 5.

Table 5. Area under different classes of aspects, slope, and river density.

Aspect	Area (%)	Slope (°)	Area (%)	River Density (m/km^2)	Area (%)
Flat	0.1	<5	4.8	<50	64.3
North	13.5	5–10	8.4	50–100	12.5
Northeast	12.3	10–20	20.8	100–200	15.7
East	11.5	20–30	27.0	200–300	6.0
Southeast	11.3	30–50	34.3	>300	1.5
South	13.0	>50	4.7		
Southwest	13.9				
West	12.7				
Northwest	11.7				

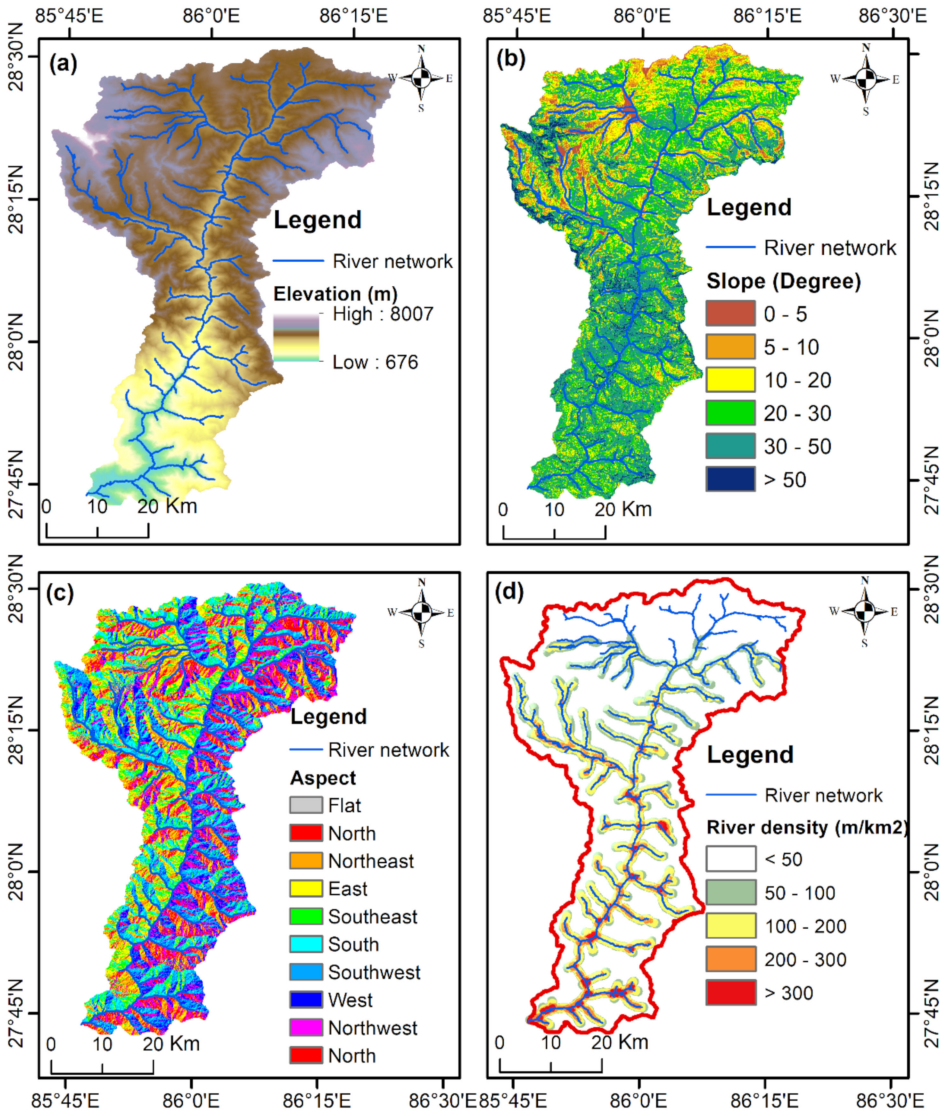

Figure 2. Topographical characteristics: (**a**) elevation, (**b**) slope, (**c**) aspect, (**d**) river density.

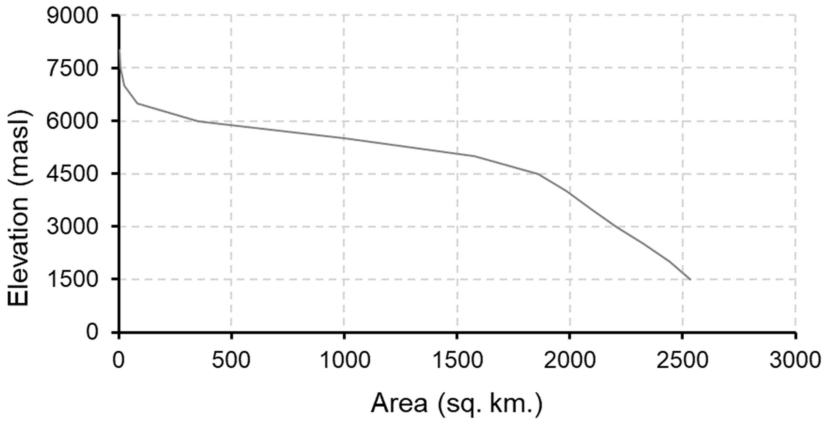

Figure 3. Hypsometric curve of the Bhotekoshi–Sunkoshi watershed.

4.2. Geological Aspects of Multihazards

4.2.1. Geological Setting

Geology and geomorphology play a significant role in the preparatory process of multiple hazards in the Himalayan region due to its high degree of fragility and greater tendency to

undergo accelerated decomposition under the influence of various climatic factors [39]. The BSW lies in the complex geological setting within the Himalayas, with all its major geological structures trending East–West (EW). The northern part of the watershed has fossiliferous sedimentary rocks from Tethyan sediments, while the central and southern parts have high to low-grade metamorphic rock from the Lesser Himalayan and Higher Himalayan sequence (Figure 4). The Main Central Thrust (MCT) and South Tibetan Detachment System (STDS) are the two major thrusts separating different the lithological units of the basin [33]. The sedimentary rocks and high-grade metamorphic rocks on the northern side are more prone to GLOF events, while low-to-medium-grade metamorphic rocks from Lesser Himalayan Sequence on southern side is prone to landslide, debris flow, and LDOF, predominantly during monsoon season. The detailed lithological characteristics of these units in the proximity to the weak geological conditions and major thrusts from the study area help us to understand better the occurrence and intensity of multiple geohazards.

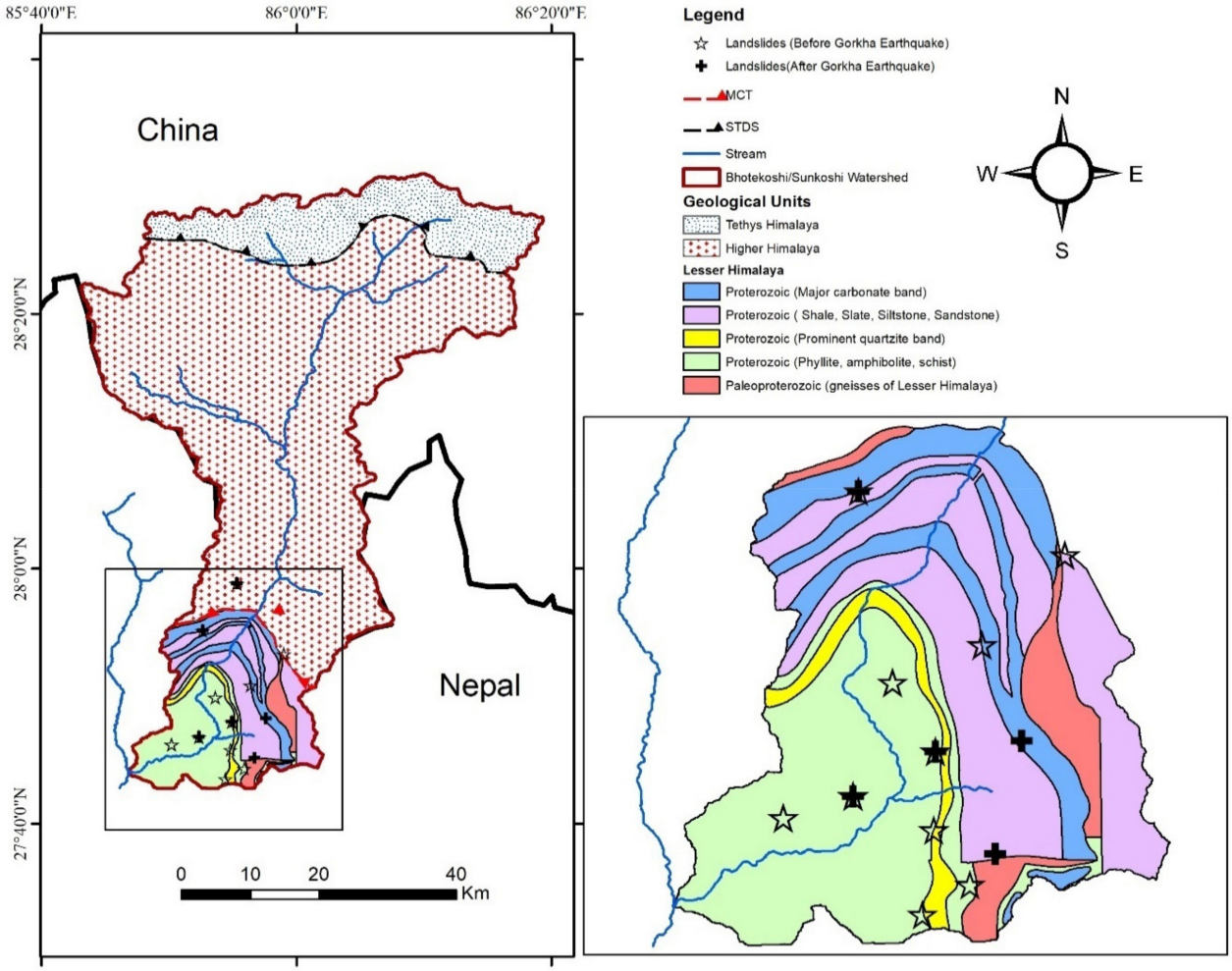

Figure 4. Geological map of the study area (modified from: [48,49]).

4.2.2. Geostructure and Lithology

The major triggering geohazards in the study area appear to be earthquakes and rainfall-induced landslide events, which lead to LDOF, upstream flooding, and GLOF as cascading hazards. The major rock type, lithology, thrusts, faults, and tectonic windows are the major geological structures affecting the events and intensity of multiple hazards in the study area. The majority of the study area is covered with a crystalline belt of high-grade metamorphic rock and granitic gneiss of Higher Himalaya separated by the MCT in the south and STDS in the north [37]. Southern part of the watershed is a part of Okhaldhunga

window, the largest tectonic window of Nepal, whereas the Lesser Himalayan rocks occupy the core of the Great Midland Antiform [50]. The presence of this unique tectonic window, together with the presence of the MCT, makes this area more vulnerable from the perspective of multiple geohazards.

The positive correlation between rock type and landslide events in the Himalaya is a well-established phenomenon, with rock types such as phyllites, shales, and schists being more susceptible to landslide compared to cemented sandstones, limestones, gneiss, granites, and quartzites [51]. The southern part of the study area, with numerous landslide events before and after the 2015 Gorkha earthquake, is concentrated within the two lithological units, Proterozoic (Phyllite, amphibolite, schist), and Proterozoic (Shale, Slate, Siltstone, Sandstone) (Figure 4). This part of the watershed has higher probability of geohazard events due to its complex geological setting with weak rock type and presence of active faults. The 2014 Jure landslide is the best example of a geohazard event where a landslide dam was formed which inundated a large upstream area with eminent threat of LDOF downstream.

Unlike rainfall-induced landslides, earthquake-induced landslides are more prone to occur at higher elevations between 2000–3000 m and 3000–4000 m and on steeper slopes with a slope gradient of 40–50° and 30–40° [52]. Landslides and debris flow events have increased lately in the southern part of the study area after the 2015 Gorkha earthquake [52]. Several landslides and LDOF events were reported lately, mostly in the Lesser Himalayan rock unit within the elevation range of 2000 m to 3000 m, which clearly suggests the probability of similar multihazard events in near future too.

4.3. Hydrometeorological Aspects of Multihazard

Rainfall can play a critical role in the development of geohazards, such as landslides, because rainfall infiltration may increase the degree of soil saturation, reduce soil shear strength, and ultimately lead to the occurrence of geohazards [45,46]. Furthermore, high intensity rainfall may lead to high flooding events, thus, taking lives and properties. Our study currently limits the analysis of long-term subdaily precipitation data. The concentrated rain during the monsoon season (June to September) results in numerous geohazards in the watershed.

The hydrological characteristics of the study area are shown in Figure 5. The spatially averaged values of the mean monthly climatic variables (rainfall, rainy days, and temperature) clearly show significant intra-annual variability. In particular, a strong seasonality in rainfall could be observed, with almost 80% of the average annual rainfall being received during the rainy season. Due to a large altitudinal variation across the study area, there are significant temperature differences between the highest temperature (over 23 °C) at lower regions during July and the lowest temperature (below −20 °C) at upper region of the study area during January. An average of 30 °C variation of temperature could be seen across the study throughout the year. The river valley is warmer and drier compared to the hill slopes. The monthly rainfall is above 350 mm (rainy days ~11 days) during July and August, accompanied by the highest air temperature (about 8 °C, varying from −4.5 °C in the upper region to 23 °C in the lower region). Generally, the heaviest rainfall is accompanied by the greatest average temperature. The monthly variation of the river discharge at Bahrabise shows a peak value during August. July and August are the two months when a peak instantaneous discharge could happen upon heavy rainfall upstream of the study area. We found that 10–13% of the annual rainfall is contributed by a single day's rainfall, which clearly indicates high-intensity, short-duration rainstorm events are recurrent across the study area. Considering the maximum consecutive seven-day rainfall for every year between 1981–2019, this study finds that about 20% of the total annual rainfall occurred during the consecutive seven-day period. Under such a scenario, the soil of the hillslopes becomes completely saturated, and there are high chances of the failure of unstable slopes. After the 2015 Gorkha earthquake, more than 2000 landslides (small to large) occurred along the corridor of Bhotekoshi–Sunkoshi River [53].

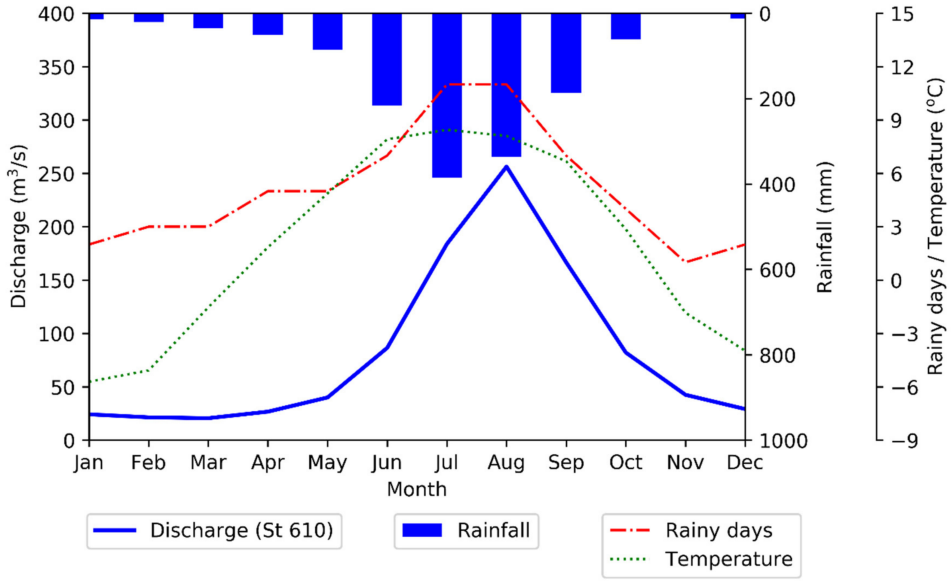

Figure 5. Mean monthly discharge at Bahrabise station (Station no.: 610) and basin-averaged mean monthly rainfall (inverted y-axis at right), and rainy days and average temperature (offset right axis) of the study area. Monthly discharge data for Bahrabise station is computed from the data maintained by the Department of Hydrology and Meteorology (DHM), basin-averaged rainfall and rainy days are computed from the CHIRPS data using 94 grid points and basin-averaged temperature is computed from the WorldClim data.

Figure 6 shows spatial distributions of mean annual precipitation, maximum one-day precipitation, and mean annual count of days when daily precipitation ≥50 mm for different four decades and the entire period (1981–2019). The mean annual precipitation (1981–2019) varies from about 1000 mm at upper region to 2700 mm at lower region of the study area with a basin-averaged value of 1450 mm. The lower region of the study area (meaning the Nepal–China border to river confluence at Balephi) receives high rainfall compared to the upper region. We chose two extreme precipitation indices (RX1day and R50) because they provide information about the locations susceptible to the high-precipitation and likely rainfall-induced geohazards. There are some locations where the number of days in a year with daily precipitation ≥50 mm (R50) is above 18 days across the lower region of the study area, meaning the location is highly susceptible to soil erosion, landslides, and resulting debris flow. There are not any particular decadal trends for selected extreme precipitation indices and annual precipitation. In general, the tendency shows a constant to slightly decreasing precipitation amount and extreme precipitation indices (average value). However, the yearly fluctuations are significant, and the decreasing tendency is mostly found in upper region of the study area. The lower region of the study area receives frequent heavy rain (i.e., R50) and recently most of the landslides have been recurrently occurring around this area.

We further characterized the average annual as well as seasonal discharge and their trends over the years based on the observed discharge at the outlet of the watershed (Bahrabise, index: 610). The average annual discharge of 1965–2006 is 81.1 m^3/s, with variations over the months from 20.6 m^3/s (in March) to 255.4 m^3/s (in August). The recorded average monthly discharge for the month of highest flow varies from 145.7 to 846.5 m^3/s. Furthermore, the instantaneous flood time series for the 35 years spanning from 1965 to 2006 ranges from 292 to 1030 m^3/s, with an average value of 614 m^3/s. Flood frequency analysis using Gumbel distribution showed that floods of the return periods 100, 500, 1000, and 10,000 floods at the outlet of the watershed are 2401 m^3/s, 3112 m^3/s, 3417 m^3/s, and 4430 m^3/s, respectively (Figure 7).

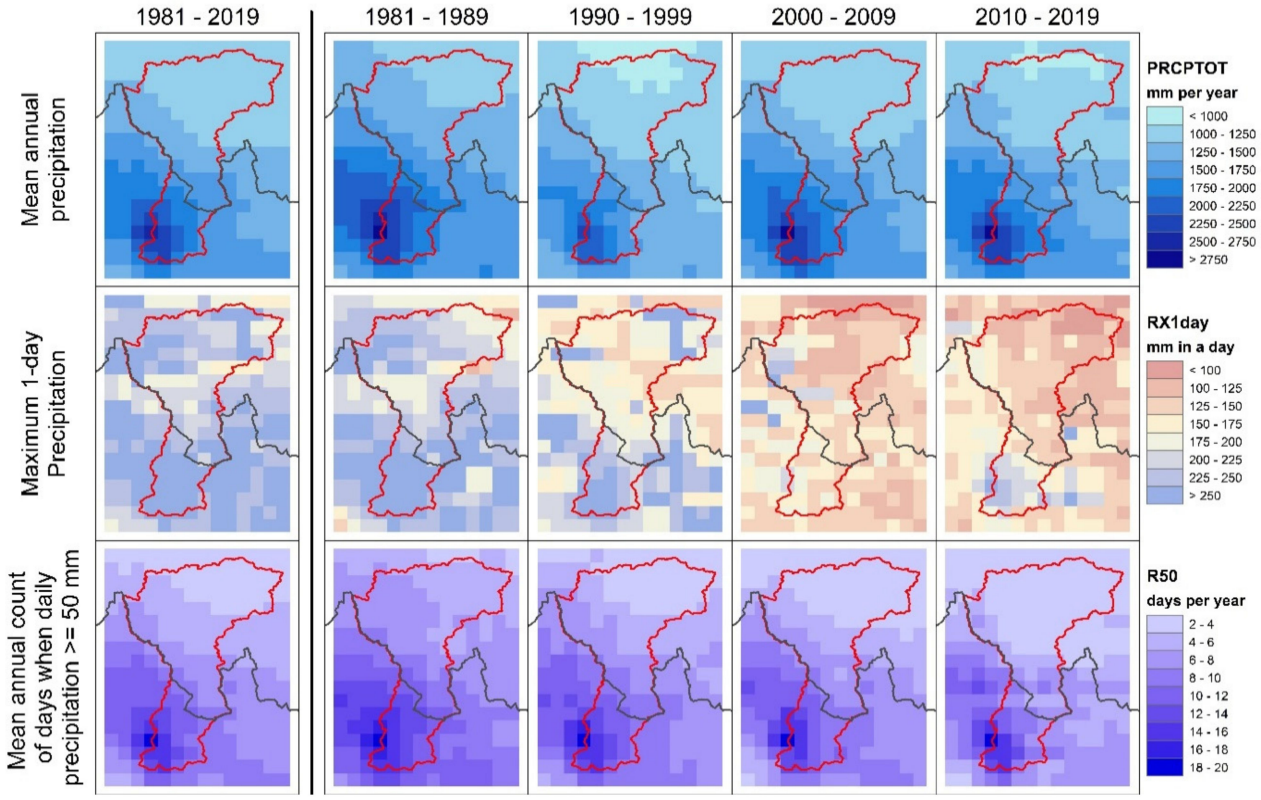

Figure 6. Spatial distributions of mean annual precipitation (at top panel), maximum 1-day precipitation (at middle panel) and mean annual count of days when daily precipitation ≥50 mm (at bottom panel) for the entire selected period (1981–2019 at the left), and for different four decades: 1981–1989, 1990–1999, 2000–2009, and 2010–2019 (left to right, respectively). The daily precipitation data are obtained from CHIRPS dataset at a spatial resolution of 0.05° (~5 km).

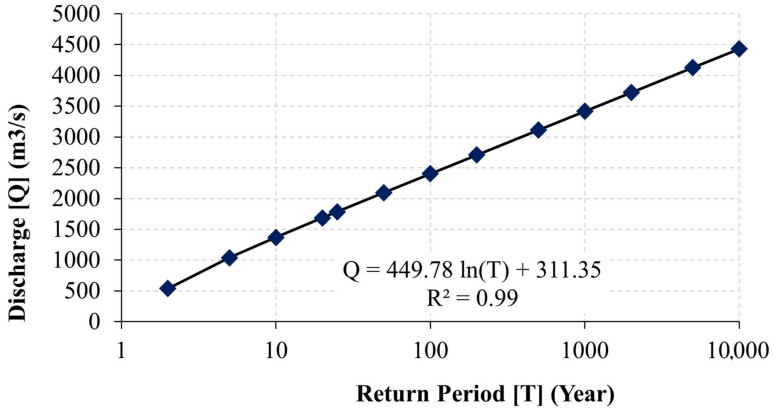

Figure 7. Floods of various return periods based on Gumbel distribution at Bahrabise station (index: 610).

4.4. Glacial Lakes—Presence and Vulnerability

Glacial lakes are precious freshwater resources in the natural landscape; they play an important role in the cryosphere and climate change and act as a trigger of many glacial hazards such as glacial lake outburst flood (GLOF) and debris flow [48]. Under global warming and associated climate change, the tendency (amount and intensity) of glacier-related hazards such as GLOF are on rise. GLOFs are of concern in this region due to several disasters causing significant loss of life and damage to infrastructures. GLOFs often originate at high elevation, in poorly inaccessible terrain and mostly transform into hyperconcentrated or debris flow and resulting subsequent flow transformation or chain reactions such as the damming of valleys, secondary outbursts, and debris flow [37]. There is a high probability of converting GLOFs into debris flow by erosion and sediment en-

trainment along a flood route and flood eroding channel bed down the valley, leading to an increase in peak discharge and volume, causing destructive damage downstream [36]. In the Sino–Nepal border region, numerous lakes, dams, parent glaciers in different topographic conditions and characteristics are in existence [37], which may outburst if triggered by any extreme climatic and geological events. This increases vulnerability and risks to people, livelihood activities, infrastructure, and other services of the watershed.

There are 124 glaciers, covering an area of 200 km^2, mapped in the study watershed. Nine of them are potentially dangerous, and all of them are located within Tibet [49]. It indicates the vulnerability of Nepali watersheds originated from Tibet to possible GLOFs. For example, the Poique watershed in Tibet, upstream of BSW, has been identified as highly prone to GLOF. The GLOF hazard in the study basin has further increased after the earthquake due to landslide deposits, which could provide abundant deposits for outburst floods to evolve as debris flow [36].

Five major GLOF events were reported in this watershed since 1935 [9]. They include the Taraco GLOF on 28 August 1935, the Zhangzambu (Ci-ren-Ma-Co) GLOF in 1961 and in 1981, and the Jia-Long Co GLOF in 2002. In addition, Jure landslide formed a lake by damming the river on 2 August 2014, at about 1.4 km upstream from the Sunkoshi Hydropower Project's headwork site. It formed a lake that extended up to 3 km upstream, completely submerging the 2.6 MW Sanima hydropower project [54]. That event damaged several agricultural fields, bridges, houses, roads, and other infrastructures. Several livestock animals and people were swept away, power was cut for a month, traffic was blocked, and trade disrupted for a month between Nepal and China, and transport services were affected for three years. The potential losses on the Nepalese side alone from a GLOF event in 1981 but with a 10 m higher dam is estimated in a range of USD 153–180 million [9].

Due to the topographical inconvenience, several satellites and remote sensing-based techniques were applied in the past to understand the features of the glaciers in the study area. Khanal et al. [9] identified and mapped 74 glacial lakes in the Bhotekoshi–Sunkoshi watershed based on Landsat EMT+ (22 October 22 2012). Among them, the lakes in the very large (>1 km^2) and large (0.25–1 km^2) categories were 4% and 19%, respectively. Shrestha et al. [55] reported 269 glacier lakes (19 in Nepal and 250 in China) with a total area of 21.09 km^2. Recently, Liu et al. [36] identified 122 glacial lakes (see Figure 8 for their locations) with areas larger than 0.01 km^2 based on GF-1 images from 2016 (http://www.cresda.com/CN/ (accessed on 17 March 2021)). These lakes cover an area of 20.38 km^2. Out of these lakes, 19 have high outburst potential, and 51 are at medium risk. Though some of the small glaciers are shrinking, particularly the smaller ones, and appear and disappear over time due to global warming [56], regular monitoring of glacial lakes, their spreading, and outburst susceptibility are pivotal to minimize risks of GLOFs in the downstream.

4.5. Socioeconomic Setting and Multihazard Dynamics

The BSW is situated in Sindhupalchowk district in central Nepal. Sindhupalchowk district occupies 1.73% (2542 km^2) of the total area of the country. Sindhupalchowk is one of the few districts in the high mountains having strategic road linkage to China, and it used to be the trade hub until 2014. In 2011, the total population of Sindhupalchowk district was 287,798. Among them, 128,351 were male, and 149,447 were female, with a sex ratio of 0.925. The average population density of Sindhupalchowk district was 113, and the average family size was 4.32 [44]. The largest Palika of Sindupalchowk is the Bhotekoshi rural municipality, which connects Nepal with the Tibet Autonomous Region of China. The Human Development Index (HDI) of the Sindhupalchowk district is 0.455, which is below the national average (0.49). Similarly, life expectancy in Sindhupalchowk district is 69.57 years. The per capita income of the district is USD 1110 as reported by the local administration. The Human Poverty Index (HPI) of the district is 38.03, which is fairly above the national average of 31.12. As the HPI is higher than the national average, it could be inferred that the district would have severer disaster impacts than expected due to socioeconomic conditions.

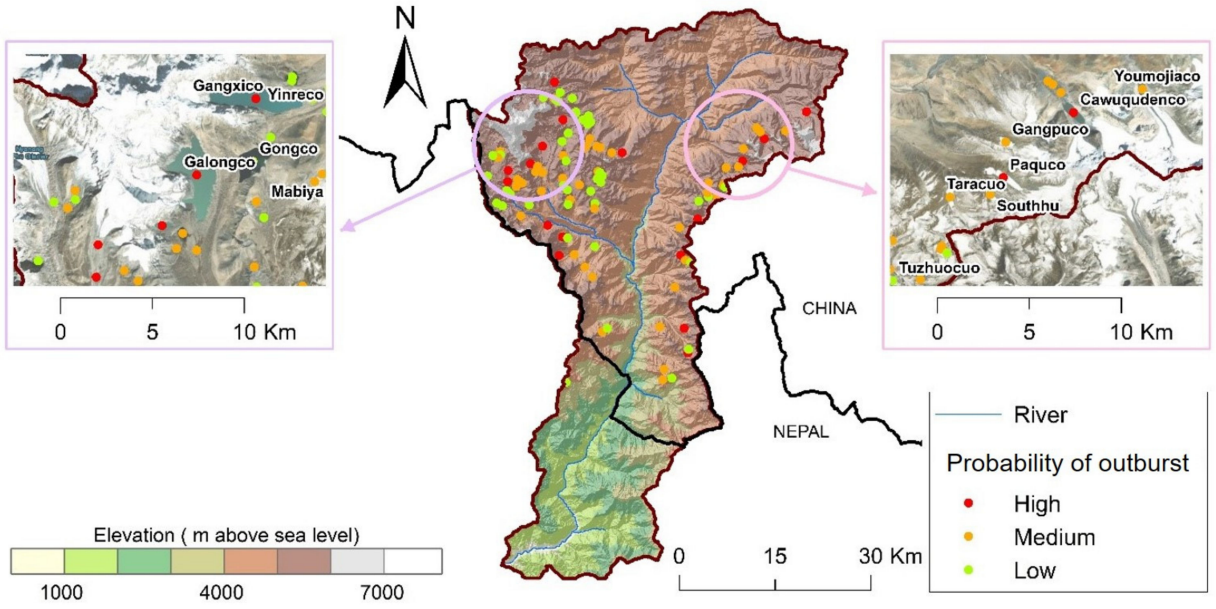

Figure 8. Location of glacial lakes (count = 108) across the study area and their probability of flood shown in three levels: high, medium, and low. The shaded is topography and hill shade. The elevation of these glacial lakes ranges from 4102 m asl (meters above sea level) to 5615 m asl. There are 17 glacial lakes with high probability of flooding. Two insets are representative areas superimposed with google image as a base map.

Agriculture is the major occupation of people in the watershed and Sindhupalchowk district as a whole. For instance, 64.52% (4935) households in Bhotekoshi rural municipality depend on subsistence farming. The major crops in the region are rice, corn, millet, and other seasonal cash crops. Due to mountainous terrain and lack of proper irrigation facilities, agriculture is just subsistence type, so food security is gravely challenged once disasters strike. Similar incidents of food security and food shortage were reported after the 2014 Jure landslide and 2015 Gorkha earthquake in this area. As per the 2011 census, there were 66,635 buildings in Sindhupalchowk district, among them 62,563 buildings were owned, 3252 were rented, and 259 were institutional buildings [44]. Among the 66,635 buildings in the district, 61,377 buildings were mud mortar masonry, 2708 were cement mortar masonry, 1322 were reinforced concrete constructions, and 651 buildings were timber constructions. The mud mortar and cement mortar masonry are highly vulnerable to several hazards such as earthquake, flood, and landslide as they do not possess adequate stiffness against the dynamic forces. Thus, in terms of building vulnerability to multiple disasters, more than 95% of buildings throughout the district are highly vulnerable. In Sindhupalchowk district, 53,799 households were dependent on pipe/tap water, 731 households were dependent on covered wells, 1264 households were dependent on uncovered wells, 9904 households were dependent on spout water, and 368 households were dependent on river/streams for water supply as per the 2011 census. As most of the households depend on tap/pipe water, the postdisaster epidemic outbreak is susceptible as, unlike the municipal supplies, tap/pipe water supplies are not treated before or after the natural disasters. Similarly, a significant fraction of the population also depends on wells, which could lead to epidemic outbreaks. The 2011 census noted that 61,407 households out of the 66,635 were dependent on firewood as the major fuel for cooking. The use of firewood has multifaceted challenges from human health to pressure on forest area. Similarly, fire hazard is expected quite often as none of the Nepali rural and periurban settlements have dedicated fire space and safe kitchens for cooking using firewood. Nearly one in three households (23,900) did not have a toilet in Sindhupalchowk district. The lack of toilets and sanitation facilities leads to disastrous cascading effects or impacts associated with cholera and dysentery outbreaks. Among the 66,635 households in Sindhupalchowk, 34,649 households had a radio, 22,599 households had a television, 395 had internet, 39,543

had a cellular phone, and 1332 had telephone facilities [44]. Thus, it is pertinent to note that any early warning or preparedness notices would be more effectively communicated via cellular phone than by any other means. However, due to lack of adequate electricity supply and the loss of functionality of electricity in the aftermath of disaster, cellular phones and other means of communications would still be challenging. Although the population in the district is sparsely scattered, this may have both positive and negative implications in risk reduction efforts. Due to the scattered population, search, rescue, and rehabilitation efforts would require more resources as coordinated responses would not be able to reach in the targeted settlements in time. On the contrary, the affected population would be lower in the scattered settlements due to physiographic and other variations and the localized nature of disaster impacts. For instance, a densely populated town will suffer more than a sparsely populated village in the case of landslide, flood, fire, and similar disasters. Coping with disasters requires the effective participation of the population. In Sindhupalchowk district, 5096 households had a single person, 9229 households had two, 10,238 households had three, 13,061 households had four, 11,808 households had five, 8757 households had six, 4228 households had seven, 2127 households had eight, and 2144 households had nine or more occupants. Disaster impact would be less in the households with a fewer person; however, in terms of counteracting, a moderate sized family would perform better than a family having too many or too few people. In Sindhupalchowk district, nearly 32% of the total population are under 14 years' age and nearly 9% of total population are aged above 60 years [46]. This indicates that the adult population is around 60%, and more than one third of the population is dependent. This factor is important for planning localized disaster prevention and response initiatives. Meanwhile, the disaster impacts would also dramatically increase due to the occurrence of a significantly large dependent population. It is worth noting that 2.3% of the total population in Sindhupalchowk district are either physically or mentally disadvantaged [44]. In facing the multidimensional challenges of multihazards, disadvantaged populations would be crucial to consider for predisaster planning during disaster search and rescue efforts, as well as postdisaster rehabilitation. In total, 98,960 people in Sindhupalchowk were reported as not be able to read and write during the 2011 census. Among them, 36,771 were male, and 62,189 were female. It is obvious that female population is more vulnerable to disasters, and a lower literacy rate would further aggravate the impacts. Owing to the literacy situation, awareness and preparedness initiatives need further dissemination considerations so that such efforts really reach the target groups.

5. Case Study of Selected Hazards

5.1. Glacial Lake Outburst Flood (GLOF)

GLOFs occur in the Himalayas mainly due to geomorphic changes and catastrophic failure of moraine dammed lake resulting in a sudden discharge of water reservoir, which is formed either underneath, at the side, in front, within, or on the surface of a glacier [37,57]. Nepal has 3624 glacial lakes in three major river basins (Koshi, Gandaki, and Karnali); among them 47 glacial lakes were identified as potentially dangerous. In the Sunkoshi basin, 181 glacial lakes with 22.13 km^2 area were recorded in 2015 [9]. Among the 47 potentially dangerous glacial lakes, 42 are in the Koshi River Basin that incorporates BSW too, and four others are situated on the Chinese side of the study area (Figure 8). Until 2020, this region experienced seven major GLOF events from four glacial lakes (see Table 6), leading to significant damage to structures and infrastructure. Wheat fields of 66,000 m^2 were damaged, and several yaks were swept away by the GLOF induced by piping and seepage on 28 August 1935 [58]. The Cirenmaco glacial lake, one of the potentially dangerous lakes, was triggered by piping action in 1964, and the next GLOF event was reported on 11 July 1981. This event was triggered by an ice avalanche. The GLOF caused the deaths of 200 people, damage to the friendship bridge (Sino–Nepal border region), 47 houses, 12 bridges, 27 km of road, and a gate of the Sunkoshi hydropower station [9]. In addition to this, the power supply was obstructed for 31 days, and trade between Nepal and China

was disrupted for 36 days due to traffic blockage, and the transport service was affected for three years. On 11 July 1981 and 23 May 2002, GLOF events were reported in the same region. These GLOF events destroyed bridges, the highway, and the hydropower station due to ice avalanche and resulted in an economic loss of approximately USD $370,000 [36]. The most recent GLOF event occurred on 5 July 2016, which was caused by the outburst of Gongbatongshotascho (GBTSC) lake in the Zhangzangbo Valley. This event caused severe damage to 77 houses, 3 bridges, and the Arniko Highway. Furthermore, it destroyed the intake dam of the Upper Bhotekoshi Hydropower Project in Nepal. The 1981 GLOF event generated maximum discharge of 15920 m^3/s, 23 min after bursting, which discharged approximately 19 million cubic meters of burst water i.e., 16 times more than the average annual flood in the Sunkoshi River [9]. It was also estimated that nearly 4 million m^3 of debris with a moving layer of 4–10 m thick sediment was carried by this event and the water level tose to 30 m, which destroyed Quxiang village on the Chinese side. The GLOF event of 5 July 2016 drained the water catastrophically, releasing approximately 1.1×10^5 m^3 from GBTSC lake [57]. The triggering mechanism is unknown for this event, but the affected area is situated in the region affected by the 2015 Gorkha earthquake. The 2016 event affected the river channel for ~40 km stretch between the confluence of the Zhangzangbo River and Bahrabise neighborhood. The study based on satellite images reported undercutting at the base of slope, downcutting varying from 1 to 10 m, and an increase in bank width.

Table 6. Historical GLOF events in study area (modified from: [37]).

Name of Lake	Date of Outburst	Latitude	Longitude	Elevation (masl)	Burst Water Volume (10^6 m^3)	Damage	Triggering Factor(s)	Reference(s)
Taracho	28 August 1935	28.29	86.13	5245	6.3	Farmlands, yaks	Damage collapsed by seepage	[49,58]
Cirenmaco	1964	28.07	86.07	4627			Piping	[49,58]
	11 July 1981				18.9	200 deaths, friendship bridge, hydropower station	Ice avalanche	[54,58]
Jialongco	23 May 2002	28.21	85.85	4374	23.6	Hydropower	Ice avalanche	[49]
	11 July 1981					Station, highway		
Gongbatongsha Tsho	5 July 2016	28.08	86.06	4608				[55]

5.2. Rainfall-Induced Landslides

5.2.1. Association of Rainfall Amount and Landslide Occurrence

A total of 47 landslides are recorded in the study area from 1981 to 2019, which were compiled using a wide range of sources, including newspaper and technical reports. Only five out of 47 landslides were reported in nonmonsoon seasons, whereas 42 landslides were reported during the monsoon season. As expected, most of the landslides were predominantly driven by rainfall. August is the month with the highest occurrence of recorded landslides (n = 23), followed by July (n = 12). Figure 9 shows a summary of rainfall amounts for different rainfall indexes for those 47 events. The average value of 24-h rainfall for the 47 events is only 18 mm, with the highest value of 51 mm. Since the same daily 24-h rainfall was taken, there might be chances that if the landslide occurred during the early morning, the rainfall recorded on that day would not directly correlate with the occurrence.

However, the cumulative rainfall derived from daily rainfall data is of great importance to understand the likely saturation level of the hill slopes. The average (maximum) values for 3-day, 5-day, 7-day, 10-day, and 20-day rainfall of these instances area are 55 mm (163 mm), 90 mm (249 mm), 123 mm (322 mm), 174 mm (402 mm), and 343 mm (668 mm), respectively.

With the information from these historical events, the likelihood of landslide events based on rainfall amounts can be estimated. As a general rule of thumb, rainfall characterization was done using the 45th to 55th percentiles as thresholds to indicate thechances of landslides across the study area (Table 7). A precise threshold estimation requires the physical-based modeling of hillslope stabilization. Further, we should pay attention to the role of soil moisture variation [59]. Remotely sensed soil moisture information is helpful for the ungauged areas [60]; however, the performance of such products should be assured before using.

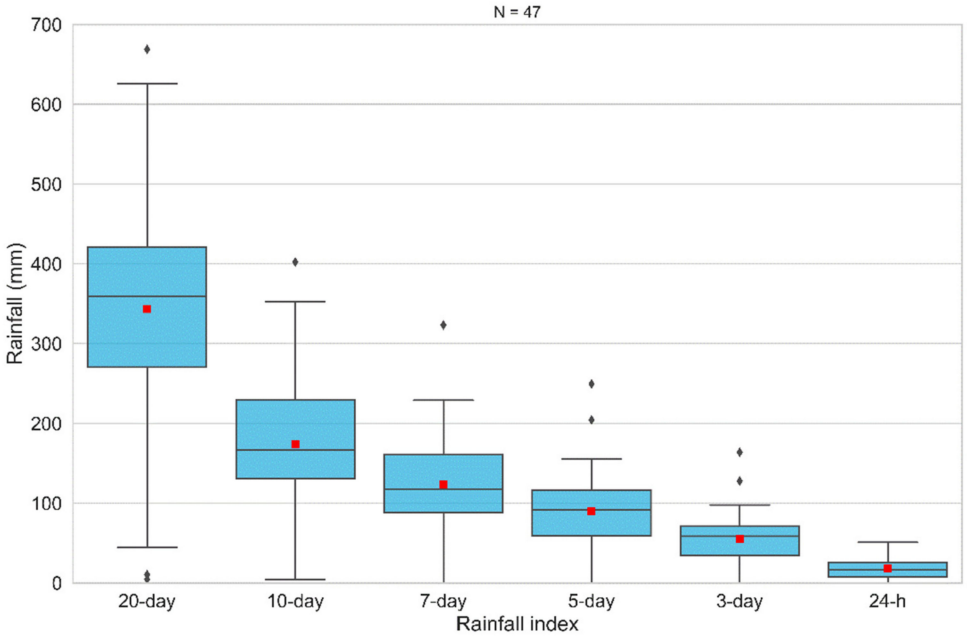

Figure 9. Boxplot showing the variation of different rainfall index based on cumulative rainfall (20-day, 10-day, 7-day, 5-day, 3-day and 24-h) before the occurrence of landslide based on daily rainfall data. No. of landslides (*n*) used in this study is 47 that occurred inside the study basin around Nepal side. Red square indicates the average value and boxplot shows quantiles (Q1 and Q3), median (Q2) and range of variation.

Table 7. Rainfall threshold for chances of occurrence of landslide across the study basin.

Rainfall (mm)					
20-Day	**10-Day**	**7-Day**	**5-Day**	**3-Day**	**24-h**
(337.6 to 379.8)	(161.5 to 189.7)	(111.3 to 129.2)	(84.6 to 98.8)	(52.1 to 62)	(0 to 51)

5.2.2. Jure Landslide (2 August 2014)

The Jure landslide, which occurred in the early hours of 2 August 2014, is one of the massive landslides in Nepal. The landslide mass (rock and debris) completely blocked the Sunkoshi River and created a landslide dam (Figure 10). The river also showed nil discharge for the first nine hours, and an outlet was opened at around 2 pm (almost 12 h of damming) by experts from government agencies and the Nepali Army [61]. After 37 days of the formation of the landslide dam and artificial lake, the dam breached on 7 September 2014, predominantly due to overtopping. During the landslide, there was no rainfall, as evidenced by the rainfall observing station at the Bahrabise gauging station located ~3.7 km upstream, which showed zero rainfall reflecting the causes behind the huge mass movement, not the exact measurement of the rainfall. However, the rain that infiltrated along the cracks and into the loose soil layer during the monsoon (rainy season) might have saturated the unstable mass. Shrestha and Nakagawa [61] reported that satellite images acquired in September 2013 showed the area had experienced landslides and several scars, revealing the existence of an unstable mass along the mountain slope. Ao et al. [62] also

revealed that the upper part of landslide had long become unstable before the collapse. Further, the expansion of nonengineered road construction is promoting shallow landslides or reactivating old landslides.

Figure 10. Jure landslide site. The photo on the left (Image credit: Narendra Khanal) shows the site after a small movement of earth in June 2013. On the right, the same site after the devastating landslide on 2 August 2014. The lake formed by the landslide dam can be observed in right image.

5.2.3. Incessant Rainfall-Triggered Mudslide/Debris Flow (9 July 2020)

Continuous monsoon rainfall from 8 to 10 July 2020 triggered multiple landslides and floods in central Nepal. More than ten houses were swept away in the Bahrabise municipality alone. The intense rainfall occurred between 11 pm (8 July) to 1 am (9 July), and the rainfall continued until 7 am on 9 July local time. The Handi Khola and Kali Khola were swollen by the incessant rains, and the mudslide/debris struck at around 1:30 am. The spatiotemporal distribution of rainfall intensity estimates derived from the satellite-based product in Figure 11. We can observe that the timing of heavy intense rainfall estimated by the IMERG does not exactly coincide with the occurrence of the mudslide/landslide, indicating that there are challenges in issuing landslide early warnings based on these products. However, the high-resolution spatial information allows the delineation of areas with different likely energies associated with the continuous downpour along the mountainous slopes. The figure shows that the extreme rainfall intensity did not last for hours but was local and concentrated for a short period. It characterizes the mountain slopes in Himalayan sub-basin and provides clear information that the unstable slopes are on the verge of movement, and a local cloud burst event could generate a massive sediment disaster. If automatic weather stations (AWSs) were equipped around the location, the instantaneous rainfall intensity and likely change in soil saturation could be tracked. The geological, hydrogeological, and soil data equally play a crucial role in predicting the factor of the safety of the mountain slopes.

The debris flow and the flooded Sunkoshi River significantly affected communities and infrastructures, as shown in Figures 12 and 13. For instance, toe cutting was observed along the river stretch that threatened several settlements and damaged retaining structures. Nearly 700 m of the highway was swept away by the debris flows and toe cutting. Two people were confirmed dead and 17 others were reported to be missing. Meanwhile, 16 houses were damaged by the debris flows. Apart from this, a bridge (Purkutte bridge) collapsed due to the flooding that occurred in the Bhotekoshi River. The Middle Bhotekoshi

Hydropower Project was also affected by the debris flow on its intake side. The debris flow also affected the warehouses of the project.

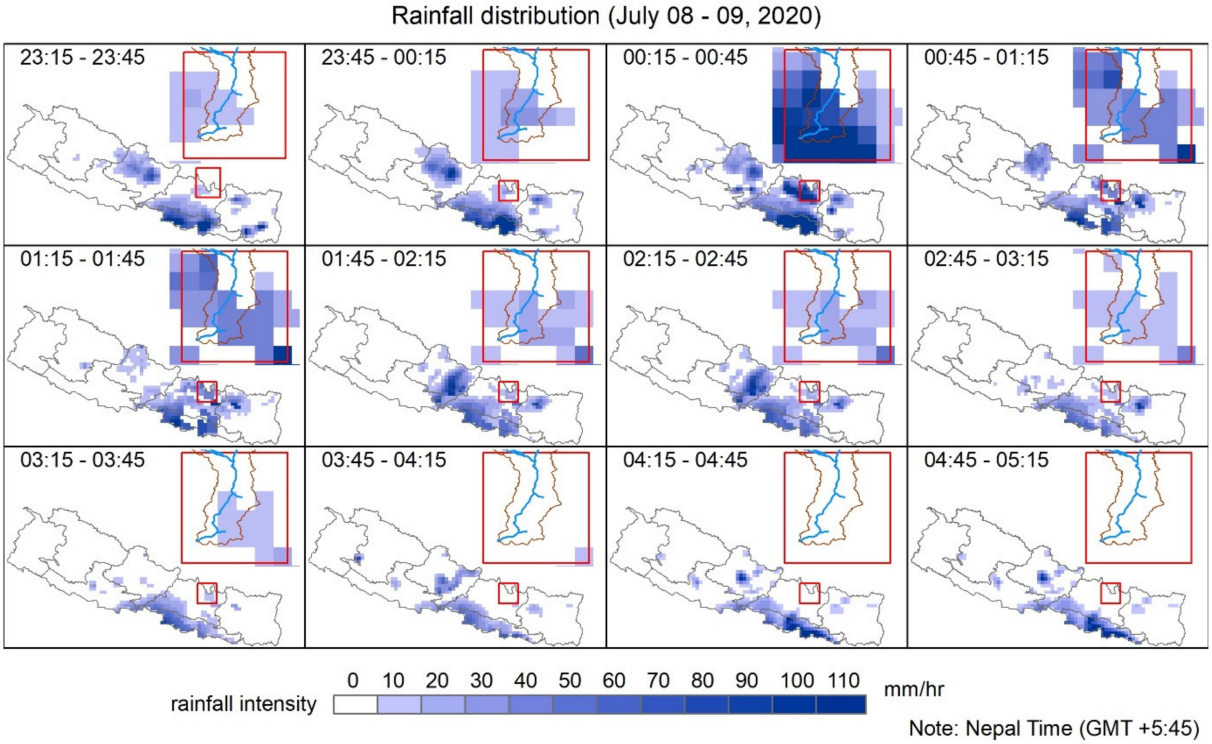

Figure 11. Spatiotemporal distribution of rainfall intensity (in mm/hr) for the period of 8 July 23:15 to 9 July 05:15 across Nepal. The rainfall intensity estimates were taken from the IMERG early product, available at a spatial resolution of ~10 km and a temporal resolution of 0.5 h. Inset at top right of each panel shows the Bhotekoshi–Sunkoshi Watershed. The disastrous mudslide/landslide and resulting debris flow occurred around 1:30 am local time.

Figure 12. Effects of flooding and debris flow: (**a**) toe cutting and subsequent damage to protection structure by Sunkoshi River, (**b**) mass movement and slope failure due to toe bank erosion, (**c**) highway section damaged due to debris flow, (**d**) flooding in Bahrabise neighborhood, (**e**) obstructed road section due to slope failure, (**f**) slope failure across a gorge.

Figure 13. (**a**) Rural road section wiped out by debris flow, (**b**) highway section damaged by debris flow, (**c**) damage to warehouse, (**d**) completely destroyed Jambu neighborhood by debris flow, (**e**) damage to Middle Bhotekoshi Hydropower Project, (**f**) widening of debris flow along the gorge.

5.3. Earthquakes

Due to the occurrence of active fault systems across the country, moderate to strong earthquakes occur frequently in Nepal and neighboring areas. The earthquake events recorded in Nepal between 1998 and 2020 are mapped in Figure 14. The earthquake events which occurred in the study area are highlighted, and a summary of the earthquake events and aftershocks is also presented in Table 8. It is noticeable that the aftershocks of the 2015 Gorkha earthquake were largely clustered in the study area. Thus, slope instability and subsequent triggering mechanisms became prominent since then. Detailed descriptions of the damage in the study area due to some notable earthquakes are presented in the following sections.

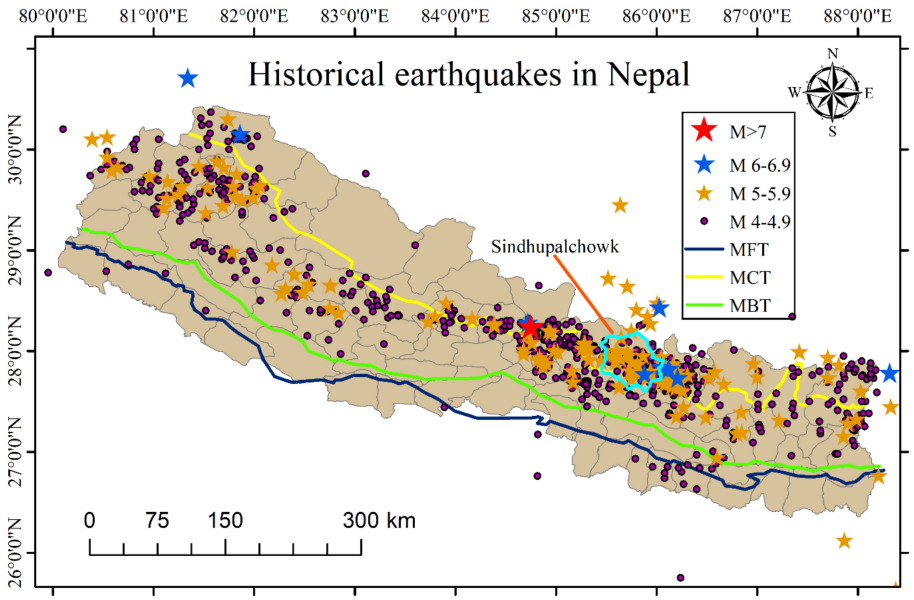

Figure 14. Earthquake events in Nepal between 1998–2020.

Table 8. Earthquakes and aftershocks with Sindhupalchowk as epicenter between 1998–2020 (modified from National Seosmological Center Nepal).

Local Magnitude (M_L)	No. of Events		Total
	Independent	Aftershock of Gorkha Earthquake	
≥6	-	1	1
5–5.9	-	17	17
4–4.9	14	131	145

5.3.1. 1934 Nepal–Bihar Earthquake

The 1934 earthquake killed 356 (4.17% of total fatalities in Nepal) in East No. 1 (present day Sindhupalchowk and Kavre districts); among them, 163 were male, and 193 were female [63]. Similarly, the earthquake collapsed 9628 and severely damaged 19,391 buildings in the then East No. 1 as reported by Rana [63]. During this earthquake, 14% of the total damage population was concentrated in East No. 1. Despite huge building damage statistics, the fatalities were relatively few, probably due to the fact that the earthquake occurred at around 2 pm and most of the people inside their houses managed to escape. Traditionally, virtually all buildings in the middle to high mountains of Nepal used to be single storied and immediate access to open space was assured in the front yard. That is why the fatalities might have been much lower than the building damage statistics because ~11% of the total collapsed buildings were in the East No. 1 region during the great Bihar–Nepal earthquake. The earthquake severely affected the Kodari region (Sino–Nepal border region), which caused extensive damage to government buildings, warehouses, military offices, and residential buildings.

5.3.2. 1988 Earthquake

The 1988 Udaypur earthquake caused two fatalities in Sindhupalchowk district, although the epicenter was located some 150 km away (for details, see [64,65]). Gupta [66] reported that 711 residential buildings and 53 public buildings completely collapsed, and 478 residential buildings and 87 public buildings sustained partial damage. Despite building damage and casualties, records of other effects such as the occurrence of landslides and secondary hazards are not available for this earthquake or for the 1934 earthquake either. This is due to the fact that the incident reporting system in Nepal was not established back then. Thus, the secondary hazards and cascading effects of the notable earthquakes are not well documented.

5.3.3. 2015 Gorkha Earthquake

The 25 April 2015 Gorkha earthquake struck mainly central Nepal and caused devastating losses in terms of fatalities, injuries, and the economy. The earthquake killed 8790 people, mostly in the 14 earthquake-affected districts in central, eastern, and western Nepal, together with some sparse casualties in other 22 districts, mostly in western Nepal [25]. Sindhupalchowk district was one of the districts most affected by the 2015 Gorkha earthquake. Sindhupalchowk was affected by almost every significant event of the 2015 Gorkha earthquake. For instance, the largest fatality of 3213 was reported due to the mainshock of 25 April 2015. Furthermore, fatalities were increased due to the 12 May aftershock of moment magnitude 7.3. Primarily, more fatalities were attributed to a highly vulnerable construction system, especially in terms of masonry buildings (stone masonry) and substandard reinforced concrete structures [67,68]. The 12 May aftershock increased the fatalities to 3440; this increase in fatalities is attributed to the collapse of already shaken structures as well as other cascading disasters such as landslides. The earthquake displayed a spectacular example of how disasters impact gender as well. In Sindhupalchowk district 1938 female and 1491 male fatalities were reported, which shows that the disasters would be more brutal towards female population rather than male. This is also attributed to the fact that most of the rural males leave their house for employment and the female population would be dominant mostly in rural areas. Apart from this, due to the engagement of most females in domestic activities, they would suffer more when disasters strike, as most of the buildings in rural Nepal are very vulnerable to natural hazards and their partial or complete collapse would result in detrimental statistics. Another interesting statistic

from the Gorkha earthquake is that injury was more prevalent in the male rather than the female population. In Sindhupalchowk district, 724 women and 844 men were injured by the Gorkha earthquake sequence. The high seismic vulnerability of the buildings is also well supported by the damage statistics. In Sindhupalchowk district, 63,885 buildings collapsed and 2751 buildings sustained partial damage [25]; notably, the total number of buildings in Sindhupalchowk was 66,688 and the population was 287,798 in 2011 [44].

Sindhupalchowk district also observed substantial damage to health facilities. The Post Disaster Needs Assessment (PDNA) reports that one hospital, one primary health center, 12 health posts, and two private sector health facilities collapsed due to the earthquake. Similarly, two primary health centers and 17 health posts sustained considerable damage. The total loss in health sector due to the Gorkha earthquake was estimated to be NRs. 559 million attributed to the damage of 456 infrastructure and other facilities [25]. The immediate operation of health facilities would be crucial to assure, especially in the case of disasters. So, the hospital infrastructure should be resilient enough and more robust than the residential buildings. However, there is no discerning health facility construction guideline in Nepal, making the health facility buildings designed and constructed in a conservative way. Although the government declared free treatment of all the injured people, the health facilities were not properly functional after the Gorkha earthquake, especially in rural areas such as Sindhupalchowk. This put additional pressure on central level engagement to airlift the critically injured people in remote areas. The adversities in terms of accessibility correlate with the lower likelihood of the timely rescue of the injured people; hence, airlifting would be the only option in the case of major disasters in Nepal. However, the sufficiency of airlifting facilities would be always constrained. Several instances of weather extremity after the mainshock were reported in some locations. Due to lack of proper hygiene in the aftermath of major disasters, the epidemic outbreak would be prominent. However, the epidemic outbreak did not become prominent in Nepal although the earthquake occurred in epidemic outbreak season. Quite a few cases of cholera outbreak were reported by local news outlets but such outbreaks were controlled in time [65]. The impact of the earthquake on children, pregnant women, and lactating women was most intensive in Sindhupalchowk district among the affected ones. At least 28,158 children of less than five years of age, 7351 pregnant women, and 6230 lactating women were directly affected by the earthquake.

The loss due to the damage of cultural heritage in Sindhupalchowk was estimated to be USD 1.5 million; similarly, the total recovery estimate was depicted to be USD 1.8 million by the National Planning Commission [25]. As reported by the National Planning Commission, the total damage to crops in the Sindhupalchowk district by the Gorkha earthquake was NRs. 1075.6 million. Similarly, the damage to livestock was NRs. 3382 million, and the agricultural damage was NRs. 4457.6 million. The earthquake affected seven irrigation systems in Sindhupalchowk leading to a total loss of NRs. 12.6 million. The total loss attributed to the damage in industry in Sindhupalchowk was NRs. 142.7 million due to losses in micro, cottage, medium, and large industries. Similarly, the total loss attributed to commerce was NRs. 134.7 million. The 2015 earthquake damaged 14 microhydro projects with an installed capacity of 123 kW. The damage affected the electricity supply in 948 households in the affected areas. The losses attributed to water supply and sanitation in Sindhupalchowk by the Gorkha earthquake were, respectively, NRs. 838.1 million and NRs. 125.3 million. As the earthquake severely affected the productive sector, Sindhupalchowk suffered heavily in terms of employment loss. The National Planning Commission reported a total 8,528,389 workdays lost leading to NRs. 1540.4 million overall loss due to loss of employment. The 2015 Gorkha earthquake damaged 105 km of the road network in Sindhupalchowk district and caused disruption of the strategic Arniko Highway until 2020. Thus, trade with China was almost nullified through the Kodari port. The total loss due to damage in transport infrastructure in Sindhupalchowk district was estimated to be NRs. 1015 million. The National Planning Commission reported that 98.03% (546) schools in Sindhupalchowk district were damaged by the earthquake, among them 2746 collapsed.

Some notable evidence displayed by the 2015 Gorkha earthquake in Sindhupalchowk is presented in Figure 15. Figure 15a shows a dense settlement at the ridge collapsed by the earthquake. Similarly, the entire settlement across the Bhotekoshi–Sunkoshi corridor was destroyed by the earthquake, as shown in Figure 15b. The earthquake also caused extensive damage to the infrastructure. Figure 15c shows the damage to a pier of the bridge at the reservoir location of the Sunkoshi hydropower project. An important piece of cascading evidence was displayed in the Jure landslide area, as shown in Figure 15d. The landslide was again triggered. Due to the reactivation of the landslide, large boulders and debris flow occurred that blocked the Arniko Highway. Similarly, the water supply infrastructure was affected by the earthquake in Sindhupalchowk. Figure 15e shows the damage caused by the earthquake in Melamchi Water Supply Project headwork site. The earthquake triggered many landslides across the Bhotekoshi–Sunkoshi watershed. However, the size of landslide was not uniform, as shown in Figure 15f.

Figure 15. (**a**) Damaged settlement across a ridgeline in Sindhupalchowk district, (**b**) destroyed settlement along the Arniko Highway in Sunkoshi–Bhotekoshi watershed, (**c**) damaged pier of the Sunkoshi hydropower project reservoir site, (**d**) reactivated Jure landslide due to the earthquake, (**e**) damage to water supply infrastructure, (**f**) landslides triggered in the mountains across the Bhotekoshi–Sunkoshi watershed.

6. Prospects of Multihazards in Bhotekoshi–Sunkoshi Watershed

As highlighted in Section 3, the occurrence of multiple natural hazards in BSW is unavoidable. However, it is crucial to note down whether the natural hazards are converted to natural disasters. The entire study area has mountainous terrain, and many locations with unstable slopes were identified earlier; landslide is prominent in the study area. The annual torrential precipitation and devouring rainfall occur within a short period, which is quite common in the study area, so landslides would be further pronounced throughout the study area. Historically, many landslide events have occurred in this region, with more also being triggered after Gorkha earthquake 2015—the details of the individual landslide and other natural disaster events are also presented. Landslide occurrence in the BSW is also supported by the fact that one of the most active seismic thrusts, i.e., the main central thrust (MCT), passes through this region and, as in the case of earthquakes such as the 1934 and 2015 events, many landslides would be triggered. Figure 16 shows the major landslides within the study area. Interestingly, most of the major landslides are marked beside the major settlement locations (marked as village in Figure 16). This paradigm highlights a likely scenario of the severe destruction of entire settlements.

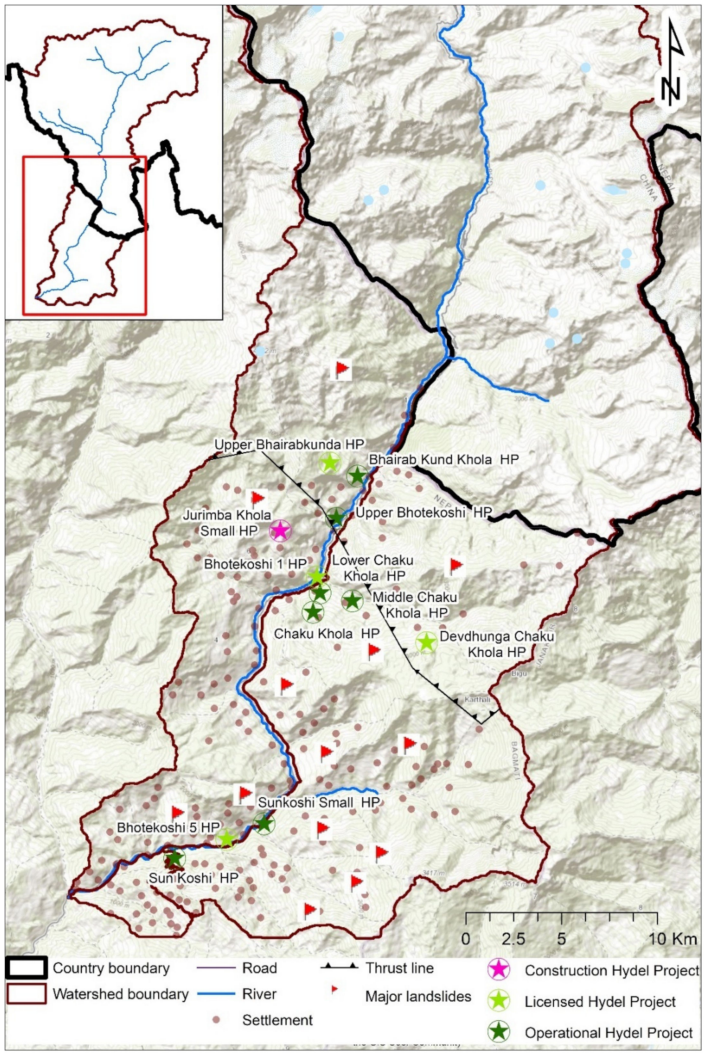

Figure 16. Built-up area of the catchment with potential sources of natural hazards and natural hazard impressions.

In terms of earthquake hazard, as the MCT passes across the study area, there is the possibility of moderate to strong earthquakes which may cause intensive damage to the structures and lifelines, as was the case during the 1934 and 2015 earthquakes. Several aftershocks of the Gorkha earthquake were reported in this region as well, and the aftershocks significantly contributed to damage aggravation of the structures and lifelines. Despite the MCT, far-field effects from other active faults may also affect the region as the residential buildings are highly vulnerable to moderate to strong shaking [68]. Earthquakes may also trigger cascading hazards such as the damming of the river network. Not only the earthquakes but the landslides usually cause damming, as in the case of 2014 Jure landslide in the study area.

The likelihood of flash floods or debris flow/mountain torrents from small streams across the steep mountain terrains is also prominent in the study area. Some cases of flooding induced by the debris flow, landslides, and damming were also reported in the past. The flash floods would cause detrimental consequences especially in the regions with steep slopes. As landslides and mountain torrents are expected in the region, flooding is also expected to occur in the low relief regions of the watershed. Several settlements, as well as the commercial centers, are situated on the banks of perennial rivers and the flash floods would also impact livelihoods as well as structures and lifelines. For instance, communication networks, basic supplies, and crops and vegetation would be affected by

flooding and other natural disasters. This situation leads to other cascading effects such as famine and epidemic outbreaks, among others.

As described in the glacier lakes categorization section, the likelihood of GLOFs is prominent in the study area. Several historical GLOF events suggest that the downstream population is affected significantly once GLOFs occur. Due to lack of early warning systems, the devastation would be unimaginable if such events were to occur during the nighttime. People need early warnings in advance at different temporal levels for different hazards such as they expect at least half an hour for safe evacuation from likely GLOF event, whereas a couple of hours or even more than a few hours warning is needed for riverine floods to safeguard both lives and properties. Furthermore, due to lack of settlement and land use planning, the expansion of the settlements on the riverbanks could be commonly observed along the Arniko Highway (shown as road in Figure 16). The inoperability of the Arniko Highway causes millions of losses every year. It is worth noting that every year the highway as well as the nearby settlements would be affected by debris flow, mountain torrents, flash floods as well as landslides. After the 2015 Gorkha earthquake, most of the displaced population settled on the riverbanks where small commercial zones were created, affecting the mobility of the highway. However, such settlements are continuously at risk of multiple natural hazards.

Despite susceptibilities to multiple natural hazards, the existence of much critical infrastructure, such as the hydropower stations, in the study area prompts more rigorous multihazard studies. As shown in Figure 16, 10 hydropower projects are either in operation or being constructed in the region where seismic activity is very frequent. The 2020 disaster incidents have proved how landslides induced by torrential rainfall and subsequent incidents affect lives, livelihoods and built environment in the study district. Owing to this sensitive scenario, stakeholders should reframe the current practices either in terms of added safety levels considering multiple natural hazards and their cascading impacts or the relocation of critical infrastructure. For example, in the case of GLOF, most of the bridge infrastructure would be swept away, as conventional bridge design and construction practice does not incorporate the scenarios that would be created by GLOF. In mountainous terrains, bridges would be easily swept away due to torrential rainfall led flash floods, as reported by Gautam and Dong [17]. The case would be more pronounced in the case of the BSW due to the fact that the Arniko Highway is one of the major lifelines that connect Nepal and China.

The socioeconomic condition of the study area is not profound as highlighted by several indexes presented in Section 3. Thus, the region is highly vulnerable to multiple disasters. For example, landslides became prominent after the 2015 Gorkha earthquake, landslides caused flooding in 2014, and so on. Thus, it is imperative to note that this particular region of the country is more susceptible of multihazards. To this end, an interdependence matrix is formulated to depict the cascading hazards in Bhotekoshi–Sunkoshi watershed. Earthquake (EQ), landslide (LS), debris flow (DF), flood (FD), GLOF (GF), and torrential rainfall (TR) are identified as the major causes of disasters in the area. The cascade matrix is presented in Table 9. As shown in Table 9, GLOF and torrential rainfall can trigger landslide, debris flow, and riverine flood in the watershed. The cascading events have become more prominent in the aftermath of the 2015 Gorkha earthquake; thus, earthquakes can also trigger landslide, flood, and GLOF events in the region. As the watershed is transboundary, attention should be paid in terms of the coordination of information exchange, especially from China. To depict the nexus between the geophysical and hydrometeorological causes and the consequences of multihazard aspects, an interrelation matrix between both natural and anthropogenic causes was developed, as shown in Figure 17. Due to the construction of nonengineered village roads, slope instabilities are quite frequent throughout the watershed. Thus, the natural disasters are being aggravated by anthropogenic activities in the watershed. The 2015 Gorkha earthquake was so prominent that almost every natural hazard occurring in the watershed would be directly related

to the cascading events and subsequent aggravation in terms of damages and losses can be observed.

Table 9. Interdependence and domino matrix for multihazard risk in the study area (EQ: earthquake; LS: landslide; DF: debris flow; FD: flood; GF: GLOF; TR: torrential rainfall); ✓: positive correlation; -: no correlation.

	EQ	LS	DF	FD	GF	TR
EQ	-	✓	-	✓	✓	-
LS	-	-	-	✓	-	-
DF	-	-	-	✓	-	-
FD	-	✓	-	-	-	-
GF	-	✓	✓	✓	-	-
TR		✓	✓	✓	-	-

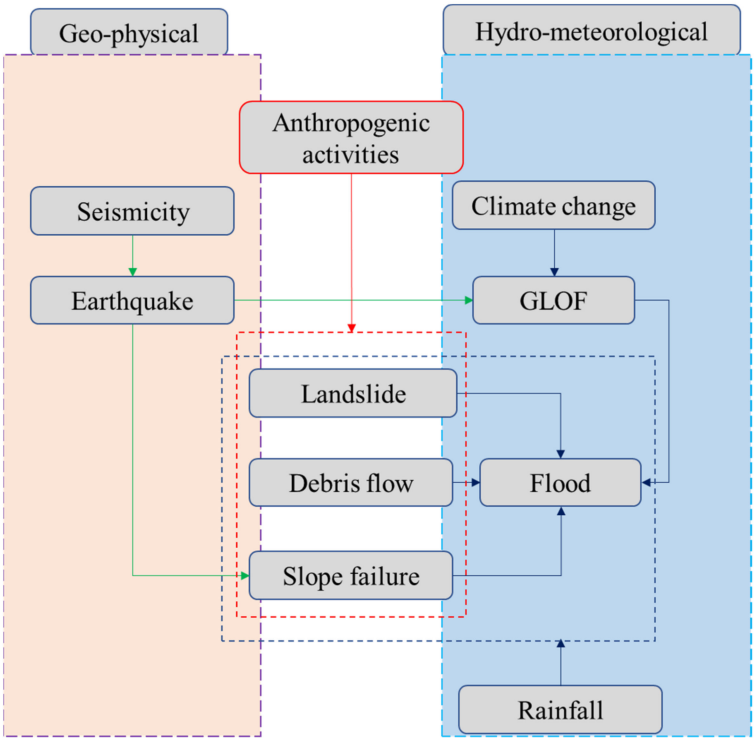

Figure 17. Cause and consequence matrix for multiple independent and cascading hazards for Bhotekoshi–Sunkoshi watershed.

7. Conclusions

Considering the Bhotekoshi–Sunkoshi watershed in the Sino–Nepal border area, geophysical, hydrometeorological, and socioeconomic characterization of the watershed to highlight the susceptibility of multihazard occurrence was performed. The topography, geology, hydrometeorology, glacial lake, and socioeconomy were identified as the major factors that either trigger the multihazards or play a vital role in the case of disasters. Based on the characterization, likely hazards were identified, and their impacts were correlated with the built environment in the study area. In doing so, all the existing and proposed critical infrastructures, human settlements, geological faults, major landslides, location of glacial lakes, among others, were mapped. The sum of observations highlights that the region will have cascading impacts after every major disaster and thus needs a holistic study covering multihazard perspectives. This study presents a new concept of watershed level characterization using geospatial techniques and multidisciplinary perspectives.

The multiple hazards nexus presented in this paper highlights cascading impacts can remarkably affect the transboundary regions. Multihazard causes and consequences are presented in terms of the cascade matrix and a framework to address the causes and consequences for mountainous transboundary watershed. The study set out to conclude that the built environment would suffer significantly due to multihazards, so policies and practices are required to be streamlined further to address localized multifaceted challenges. Historical case studies and damage and loss statistics highlight that mountainous regions will be more prominent than any other areas in terms of both independent and cascading multihazards. Quantitative study is under development for the region so as to demarcate the areas under threat of intense multihazard effects. The study will conjecture the entire watershed in terms of the habitable and nonhabitable areas and will lead to policy shifts regarding infrastructure development and subsequent precautions. More detailed study is planned to quantify the cascading scenario-based multihazard risk assessment of the region as the nexus of multiple independent hazards is quite complex and cascades have added further complexity at this juncture.

Author Contributions: Conceptualization, S.L., K.R.A., V.P.P. and D.G.; methodology, V.P.P. and D.G.; validation, V.P.P., R.T. and D.G.; formal analysis, S.L. and D.G.; investigation, S.L., R.A., V.P.P. and D.G.; resources, K.R.A., R.T., B.R.T., R.A. and A.K.; data curation, R.T., B.R.T. and R.A.; writing—original draft preparation, S.L. and D.G.; writing—review and editing, K.R.A., R.T., B.R.T., R.A., A.K. and V.P.P.; visualization, K.R.A., A.K., R.A., V.P.P. and D.G.; supervision, V.P.P. and D.G. All authors have read and agreed to the published version of the manuscript.

Funding: This research received no external funding.

Institutional Review Board Statement: Not applicable.

Informed Consent Statement: Not applicable.

Acknowledgments: The authors gratefully acknowledge generous philanthropic support from the Office of the Vice President of the Rabdan Academy, The United Arab Emirates (UAE), Nepal Academy of Science and Technology (NAST), International Water Management Institute (IWMI), Interdisciplinary Research institute for Sustainability (IRIS), and Digicon Engineering Consult for this research.

Conflicts of Interest: The authors declare no conflict of interest.

References

1. UNDP. Reducing Disaster Risk: A Challenge for Development. 2004. Available online: https://www.undp.org/content/undp/en/home/librarypage/crisis-prevention-and-recovery/reducing-disaster-risk--a-challenge-for-development.html (accessed on 7 August 2020).
2. Government of Nepal. DRR Portal Nepal. 2020. Available online: http://www.drrportal.gov.np/ (accessed on 7 August 2020).
3. Aryal, K.R. The history of disaster incidents and impacts in Nepal 1900–2005. *Int. J. Disaster Risk Sci.* **2012**, *3*, 147–154. [CrossRef]
4. Ram, T.D.; Wang, G. Probabilistic seismic hazard analysis in Nepal. *Earthq. Eng. Eng. Vib.* **2013**, *12*, 577–586. [CrossRef]
5. Rahman, M.; Bai, L. Probabilistic seismic hazard assessment of Nepal using multiple seismic source models. *Earth Planet. Phys.* **2018**, *2*, 327–341. [CrossRef]
6. Thapa, S.; Shrestha, A.; Lamichhane, S.; Adhikari, R.; Gautam, D. Catchment-scale flood hazard mapping and flood vul-nerability analysis of residential buildings: The case of Khando River in eastern Nepal. *J. Hydrol. Reg. Stud.* **2020**, *30*, 100704. [CrossRef]
7. Mishra, B.K.; Herath, S. Assessment of Future Floods in the Bagmati River Basin of Nepal Using Bias-Corrected Daily GCM Precipitation Data. *J. Hydrol. Eng.* **2015**, *20*, 05014027. [CrossRef]
8. Sharma, R.H.; Shakya, N.M. Hydrological changes and its impact on water resources of Bagmati watershed. *Nepal. J. Hydrol.* **2006**, *327*, 315–322. [CrossRef]
9. Khanal, N.R.; Hu, J.-M.; Mool, P. Glacial lake outburst flood risk in the Poiqu/Bhote Koshi/Sun Koshi river basin in the Central Himalayas. *Mt. Res. Dev.* **2015**, *35*, 351. [CrossRef]
10. Fujita, K.; Sakai, A.; Takenaka, S.; Nuimura, T.; Surazakov, A.B.; Sawagaki, T.; Yamanokuchi, T. Potential flood volume of Himalayan glacial lakes. *Nat. Hazards Earth Syst. Sci.* **2013**, *13*, 1827–1839. [CrossRef]
11. Devkota, K.C.; Regmi, A.D.; Pourghasemi, H.R.; Yoshida, K.; Pradhan, B.; Ryu, I.C.; Dhital, M.R.; Althuwaynee, O.F. Landslide susceptibility mapping using certainty factor, index of entropy and logistic regression models in GIS and their comparison at Mugling–Narayanghat road section in Nepal Himalaya. *Nat. Hazards* **2013**, *65*, 135–165. [CrossRef]

12. Yu, B.; Chen, F.; Xu, C. Landslide detection based on contour-based deep learning framework in case of national scale of Nepal in 2015. *Comput. Geosci.* **2020**, *135*, 104388. [CrossRef]
13. Gautam, D.; Adhikari, R.; Jha, P.; Rupakhety, R.; Yadav, M. Windstorm vulnerability of residential buildings and infra-structures in south-central Nepal. *J. Wind Eng. Ind. Aerodyn.* **2020**, *198*, 104113. [CrossRef]
14. Khatiwada, K.R.; Pandey, V.P. Characterization of hydro-meteorological drought in Nepal Himalaya: A case of Karnali River Basin. *Weather Clim. Extremes* **2019**, *26*, 100239. [CrossRef]
15. Adhikari, R.; Gautam, D.; Jha, P.; Aryal, B.; Ghalan, K.; Rupakhety, R.; Dong, Y.; Rodrigues, H.; Motra, G. Bridging Multi-hazard Vulnerability and Sustainability: Approaches and Applications to Nepali Highway Bridges. In *Resilient Structures and Infrastructure*; Springer International Publishing: Berlin/Heidelberg, Germany, 2019; pp. 361–378.
16. Gautam, D.; Thapa, S.; Pokhrel, S.; Lamichhane, S. Local level multi-hazard zonation of Nepal. *Geomat. Nat. Hazards Risk* **2021**, *12*, 405–423. [CrossRef]
17. Gautam, D.; Dong, Y. Multi-hazard vulnerability of structures and lifelines due to the 2015 Gorkha earthquake and 2017 central Nepal flash flood. *J. Build. Eng.* **2018**, *17*, 196–201. [CrossRef]
18. Pandey, R.; Kala, S.; Pandey, V.P. Assessing climate change vulnerability of water at household level. *Mitig. Adapt. Strat. Glob. Chang.* **2014**, *20*, 1471–1485. [CrossRef]
19. Artioli, E.; Battaglia, R.; Tralli, A. Emilia 2012 earthquake and the need of accounting for multi-hazard design paradigm for strategic infrastructures. *Eng. Struct.* **2017**, *140*, 353–372. [CrossRef]
20. Pickard, C.J.; Needs, R.J. Structures at high pressure from random searching. *Phys. Status Solidi* **2009**, *246*, 536–540. [CrossRef]
21. McCullough, M.C.; Kareem, A.; Donahue, A.S.; Westerink, J.J. Structural Damage Under Multiple Hazards in Coastal Environments. *J. Disaster Res.* **2013**, *8*, 1042–1051. [CrossRef]
22. Liu, B.; Xu, W. Comprehensive multi-risk assessment of natural hazards to human life in yangtze river delta region. *J. Nat. Disasters* **2012**, *21*, 56–63.
23. Georgescu, E.-S.; Gociman, C.O.; Craifaleanu, I.-G.; Georgescu, M.S.; Moscu, C.I.; Dragomir, C.S.; Dobre, D. Multi-Hazard Scenarios and Impact Mapping for a Protected Built Area in Bucharest, as a Base for Emergency Planning. In Proceedings of the International Conference on Dynamics of Disasters, Kalamata, Greece, 29 June–2 July 2015; pp. 57–70.
24. Santos-Santiago, M.A.; Ruiz, S.E.; Valenzuela-Beltrán, F. Multihazard risk assessment (seismic and wind) for buildings with dampers in Mexico city. In Proceedings of the 11th National Conference on Earthquake Engineering 2018, NCEE 2018: Inte-grating Science, Engineering, and Policy, Los Angeles, CA, USA, 25–29 June 2018.
25. National Planning Commission. Post disaster need assessment. 2015. Available online: https://www.npc.gov.np/images/category/PDNA_volume_BFinalVersion.pdf (accessed on 22 June 2018).
26. Government of Nepal. Nepal Flood 2017: Post Flood Recovery Needs Assessment 2017. Available online: https://www.npc.gov.np/images/category/PFRNA_Report_Final.pdf (accessed on 13 May 2019).
27. Da Silva, L.P.B.; Hussein, H. Production of scale in regional hydropolitics: An analysis of La Plata River Basin and the Guarani Aquifer System in South America. *Geoforum* **2019**, *99*, 42–53. [CrossRef]
28. Conker, A.; Hussein, H. Hydropolitics and issue-linkage along the Orontes River Basin: An analysis of the Lebanon–Syria and Syria–Turkey hydropolitical relations. *Int. Environ. Agreem. Politi Law Econ.* **2020**, *20*, 103–121. [CrossRef]
29. Hussein, H.; Grandi, M. Dynamic political contexts and power asymmetries: The cases of the Blue Nile and the Yarmouk Rivers. *Int. Environ. Agreem. Politi Law Econ.* **2017**, *17*, 795–814. [CrossRef]
30. Karki, R.; Talchabhadel, R.; Aalto, J.; Baidya, S.K. New climatic classification of Nepal. *Theor. Appl. Clim.* **2015**, *125*, 799–808. [CrossRef]
31. HLyu, H.M.; Shen, J.S.; Arulrajah, A. Assessment of geohazards and preventative countermeasures using AHP incorpo-rated with GIS in Lanzhou, China. *Sustainability* **2018**, *10*, 304.
32. Alkhasawneh, M.S.; Ngah, U.K.; Tay, L.T.; Isa, N.A.M.; Al-Batah, M.S. Determination of Important Topographic Factors for Landslide Mapping Analysis Using MLP Network. *Sci. World J.* **2013**, *2013*, 1–12. [CrossRef]
33. Auden, J.B.; Gansser, A. Geology of the Himalayas. *Geogr. J.* **1967**, *133*, 84. [CrossRef]
34. Neupane, B.; Ju, Y.; Allen, C.M.; Das Ulak, P.; Han, K. Petrography and provenance of Upper Cretaceous–Palaeogene sandstones in the foreland basin system of Central Nepal. *Int. Geol. Rev.* **2017**, *60*, 135–156. [CrossRef]
35. Nepal, N.; Chen, J.; Chen, H.; Wang, X.; Sharma, T.P.P. Assessment of landslide susceptibility along the Araniko Highway in Poiqu/Bhote Koshi/Sun Koshi Watershed, Nepal Himalaya. *Prog. Disaster Sci.* **2019**, *3*, 100037. [CrossRef]
36. Liu, M.; Chen, N.; Zhang, Y.; Deng, M. Glacial lake inventory and lake outburst flood/debris flow hazard assessment after the Gorkha earthquake in the Bhote Koshi Basin. *Water* **2020**, *12*, 464. [CrossRef]
37. Allen, S.K.; Zhang, G.; Wang, W.; Yao, T.; Bolch, T. Potentially dangerous glacial lakes across the Tibetan Plateau revealed using a large-scale automated assessment approach. *Sci. Bull.* **2019**, *64*, 435–445. [CrossRef]
38. DGautam, D. Assessment of social vulnerability to natural hazards in Nepal. *Nat. Hazards Earth Syst. Sci.* **2017**, *17*, 2313–2320. [CrossRef]
39. Dahal, R.K.; Hasegawa, S.; Nonomura, A.; Yamanaka, M.; Dhakal, S.; Paudyal, P. Predictive modelling of rainfall-induced landslide hazard in the Lesser Himalaya of Nepal based on weights-of-evidence. *Geomorphology* **2008**, *102*, 496–510. [CrossRef]
40. Fick, S.E.; Hijmans, R.J. WorldClim 2: New 1-km spatial resolution climate surfaces for global land areas. *Int. J. Climatol.* **2017**, *37*, 4302–4315. [CrossRef]

41. Talchabhadel, R.; Karki, R. Assessing climate boundary shifting under climate change scenarios across Nepal. *Environ. Monit. Assess.* **2019**, *191*, 520. [CrossRef] [PubMed]
42. Funk, C.; Verdin, A.; Michaelsen, J.; Peterson, P.; Pedreros, D.; Husak, G. A global satellite-assisted precipitation climatology. *Earth Syst. Sci. Data* **2015**, *7*, 275–287. [CrossRef]
43. Talchabhadel, R.; Aryal, A.; Kawaike, K.; Yamanoi, K.; Nakagawa, H.; Bhatta, B.; Karki, S.; Thapa, B.R. Evaluation of precipitation elasticity using precipitation data from ground and satellite-based estimates and watershed modeling in Western Nepal. *J. Hydrol. Reg. Stud.* **2021**, *33*, 100768. [CrossRef]
44. Central Bureau of Statistics Nepal. *National Population and Housing Census 2011*; Government of Nepal: Kathmandu, Nepal, 2012.
45. Xu, Y.-S.; Shen, S.-L.; Ren, D.-J.; Wu, H.-N. Analysis of Factors in Land Subsidence in Shanghai: A View Based on a Strategic Environmental Assessment. *Sustainability* **2016**, *8*, 573. [CrossRef]
46. Tian, H.; Nan, H.; Yang, Z. Select landslide susceptibility main affecting factors by multi-objective optimization algorithm. In Proceedings of the 2010 Sixth International Conference on Natural Computation, Yantai, China, 10–12 August 2010; Volume 4, pp. 1830–1833.
47. Liu, R.; Chen, Y.; Wu, J.; Gao, L.; Barrett, D.; Xu, T.; Li, L.; Huang, C.; Yu, J. Assessing spatial likelihood of flooding hazard using naïve Bayes and GIS: A case study in Bowen Basin, Australia. *Stoch. Environ. Res. Risk Assess.* **2016**, *30*, 1575–1590. [CrossRef]
48. Yao, X.; Liu, S.; Han, L.; Sun, M.; Zhao, L. Definition and classification system of glacial lake for inventory and hazards study. *J. Geogr. Sci.* **2018**, *28*, 193–205. [CrossRef]
49. Chen, X.-Q.; Cui, P.; Li, Y.; Yang, Z.; Qi, Y.-Q. Changes in glacial lakes and glaciers of post-1986 in the Poiqu River basin, Nyalam, Xizang (Tibet). *Geomorphology* **2007**, *88*, 298–311. [CrossRef]
50. Dhital, M.R. *Geology of the Nepal Himalaya: Regional Perspective of the Classic Collided Orogen*; Springer: Berlin/Heidelberg, Germany, 2015.
51. Gerrard, J. The landslide hazard in the Himalayas: Geological control and human action. *Geomorphology* **1994**, *10*, 221–230. [CrossRef]
52. Zhang, J.-Q.; Liu, R.-K.; Deng, W.; Khanal, N.R.; Gurung, D.R.; Murthy, M.S.R.; Wahid, S. Characteristics of landslide in Koshi River Basin, Central Himalaya. *J. Mt. Sci.* **2016**, *13*, 1711–1722. [CrossRef]
53. Guo, C.-W.; Huang, Y.-D.; Yao, L.-K.; Alradi, H. Size and spatial distribution of landslides induced by the 2015 Gorkha earthquake in the Bhote Koshi river watershed. *J. Mt. Sci.* **2017**, *14*, 1938–1950. [CrossRef]
54. Liu, J.-J.; Cheng, Z.-L.; Su, P.-C. The relationship between air temperature fluctuation and Glacial Lake Outburst Floods in Tibet, China. *Quat. Int.* **2014**, *321*, 78–87. [CrossRef]
55. Nie, Y.; Liu, Q.; Wang, J.; Zhang, Y.; Sheng, Y.; Liu, S. An inventory of historical glacial lake outburst floods in the Himalayas based on remote sensing observations and geomorphological analysis. *Geomorphology* **2018**, *308*, 91–106. [CrossRef]
56. Shrestha, F.; Gao, X.; Khanal, N.R.; Maharjan, S.B.; Shrestha, R.B.; Wu, L.-Z.; Mool, P.K.; Bajracharya, S.R. Decadal glacial lake changes in the Koshi basin, central Himalaya, from 1977 to 2010, derived from Landsat satellite images. *J. Mt. Sci.* **2017**, *14*, 1969–1984. [CrossRef]
57. Cook, K.L.; Andermann, C.; Gimbert, F.; Adhikari, B.R.; Hovius, N. Glacial lake outburst floods as drivers of fluvial erosion in the Himalaya. *Science* **2018**, *362*, 53–57. [CrossRef]
58. Xu, D.M.; Liu, C.H.; Feng, Q.H. Dangerous glacial lake and outburst features in Xizang Himalayas. *Acta Geogr. Sin.* **1989**, *44*, 345–352.
59. Wicki, A.; Lehmann, P.; Hauck, C.; Seneviratne, S.I.; Waldner, P.; Stähli, M. Assessing the potential of soil moisture measurements for regional landslide early warning. *Landslides* **2020**, *17*, 1881–1896. [CrossRef]
60. Zhuo, L.; Dai, Q.; Han, D.; Chen, N.; Zhao, B.; Berti, M. Evaluation of Remotely Sensed Soil Moisture for Landslide Hazard Assessment. *IEEE J. Sel. Top. Appl. Earth Obs. Remote Sens.* **2019**, *12*, 162–173. [CrossRef]
61. Shrestha, B.B.; Nakagawa, H. Hazard assessment of the formation and failure of the Sunkoshi landslide dam in Nepal. *Nat. Hazards* **2016**, *82*, 2029–2049. [CrossRef]
62. Ao, M.; Zhang, L.; Dong, Y.; Su, L.; Shi, X.; Balz, T.; Liao, M. Characterizing the evolution life cycle of the Sunkoshi landslide in Nepal with multi-source SAR data. *Sci. Rep.* **2020**, *10*, 1–12. [CrossRef]
63. Rana, B. *The Great Earthquake of Nepal*; Jorganesh Press: Kathmandu, Nepal, 1935.
64. Gautam, D.; Chaulagain, H. Structural performance and associated lessons to be learned from world earthquakes in Nepal after 25 April 2015 (MW 7.8) Gorkha earthquake. *Eng. Fail. Anal.* **2016**, *68*, 222–243. [CrossRef]
65. Gautam, D. Unearthed lessons of 25 April 2015 Gorkha earthquake (M W 7.8): Geotechnical earthquake engineering per-spectives. Geomat. *Nat. Hazards Risk* **2017**, *8*, 1358–1382. [CrossRef]
66. Gupta, S.P. *Report on Eastern Nepal Earthquake 21 August 1988: Damages and Recommendations for Repairs and Reconstruction*; Asian Disaster Preparedness Center: Bangkok, Thailand, 1988.
67. Gautam, D.; Fabbrocino, G.; de Magistris, F.S. Derive empirical fragility functions for Nepali residential buildings. *Eng. Struct.* **2018**, *171*, 617–628. [CrossRef]
68. Gautam, D. Observational fragility functions for residential stone masonry buildings in Nepal. *Bull. Earthq. Eng.* **2018**, *16*, 4661–4673. [CrossRef]